Figure 5. Number of the ES-iPS-DMRs and ES-parent-DMRs with passaging. (*A*) Number of the ES-iPS-DMRs with passaging. Red line plots indicate total number of the ES-iPS-DMRs. Blue bars indicate the number of the ES-iPS-DMRs that appeared at the earliest passage. Orange, green and red bars indicate the number of the ES-iPS-DMRs that appeared secondarily at later passages. Appearance/disappearance of the ES-iPS-DMRs and inherited regions were repeated, but the number of newly-appeared ES-iPS-DMRs was decreased with passaging. (*B*) Number of the ES-parent-DMRs with passaging. Blue bars indicate the number of the ES-parent-DMRs at P5 (or P7). Orange and green bars indicate de novo ES-parent-DMRs at P11 and P16, respectively.
doi:10.1371/journal.pgen.1002085.g005

with different parent cell types, but the numbers were consistent among iPSC clones after a 42-week cultivation. The quantity (or number) of ES-iPS-DMRs would be another validation index for iPSC identity as well as quality analysis (or methylation ratio) of pluripotent stem cell-specific methylation.

Abnormalities of imprint genes, *MEG3* genes, and *H19* genes in human iPSCs

Genomic imprinting of *H19*, *IGF2* and *MEG3* has been reported to be unstable in human ESCs [37,38]. The *Dlk1-Dio3* genes were aberrantly silenced in most of the mouse iPSC lines. But mouse iPSCs without *MEG3* expression still have the ability to differentiate into cell type of three germ layers *in vitro* [39]. In humans, IG-DMR and MEG3-DMR are relevant to upd(14)pat-like and upd(14)mat-like phenotypes [40]. In this study, only *MEG3* and *H19*, out of 87 imprinted genes examined showed aberrant methylation in human iPSCs (Figure S10). Six out of 15 human iPSC lines were aberrantly methylated at MEG3-DMR. *MEG3* expression was silenced in those six lines regardless of their parent cell type, although all parent cells showed about 50% methylation at MEG3-DMR and expression of *MEG3* (Figure S10A, S10B). However, MEG3-negative iPS lines are almost indistinguishable from MEG3-positive iPS lines in DNA methylation and gene expression in human. Continuous passaging

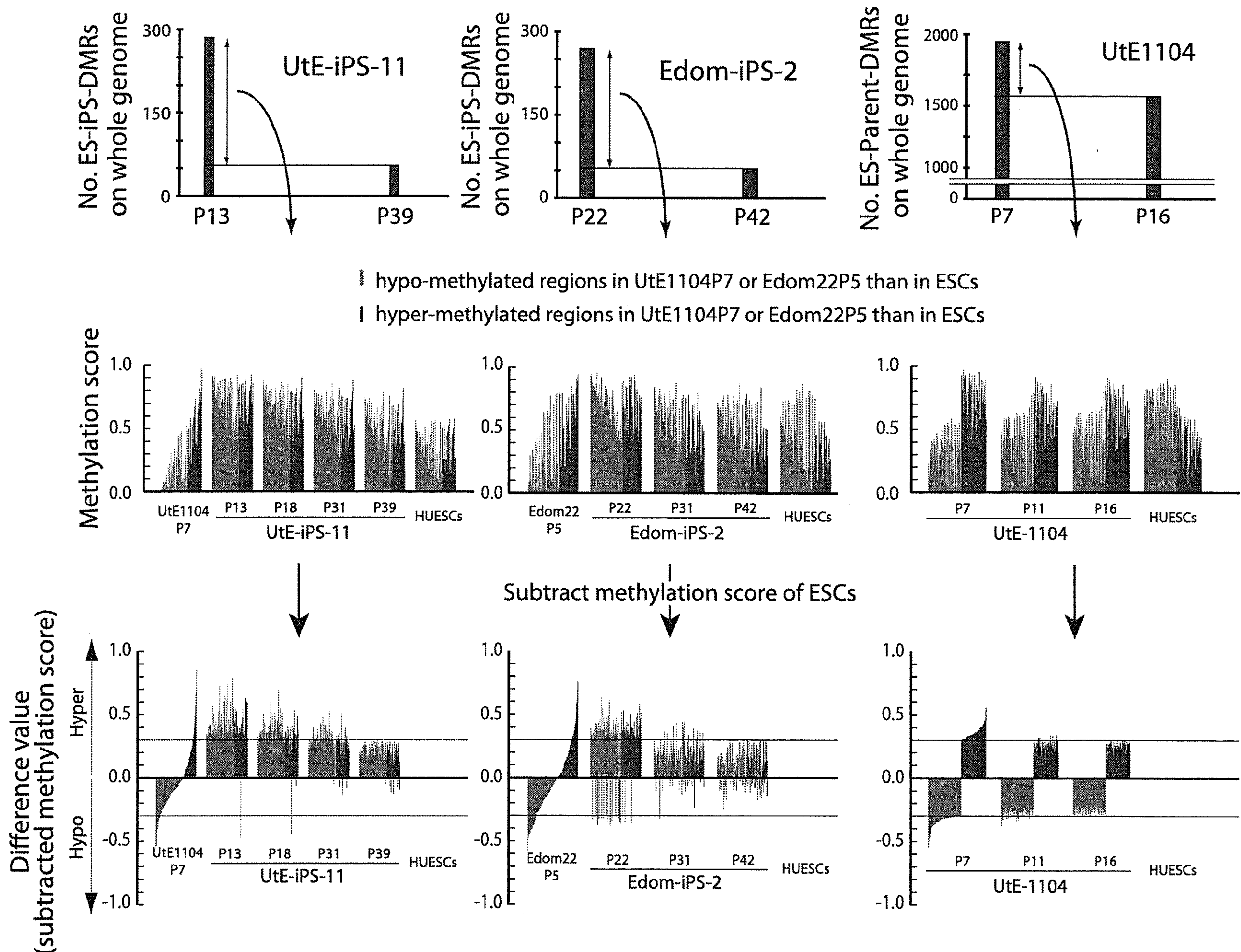

Figure 6. Hyper-methylation in the ES-iPS-DMRs and ES-parent-DMRs. ES-iPS-DMRs that disappeared in UtE-iPS-11 and Edom-iPS-2 at the latest passage (upper) were analyzed and the methylation score of each ES-iPS-DMR was plotted on bar graph (middle). To clearly compare methylation scores, difference value were estimated by subtracting the scores of ESCs from that of each sample (lower). Red and blue bars represent hypo- and hyper-methylated regions, respectively, in the parent cells, compared with ESCs. Notably, almost all the regions, even though their difference values were hypo-methylated in the parent cells, became hyper-methylated in iPSCs at the early passage, and then their methylation levels were adjusted to the level of ESCs with passaging, i.e. subtracted methylation score became close to zero. This transiently-induced hyper-methylation was not detected in parent cells.
doi:10.1371/journal.pgen.1002085.g006

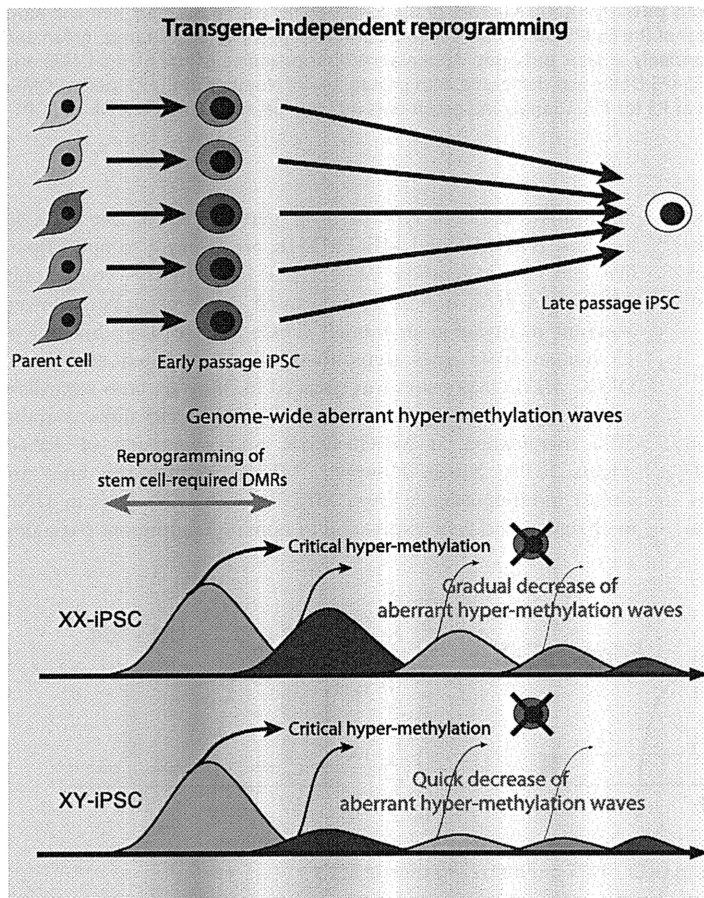

Figure 7. Model of mechanism for transgene-independent reprogramming. During reprogramming from somatic cells to iPSCs, the cells undergo dynamic change of methylation of SS-DMRs and genome. The cells with incomplete reprogramming or excessive hyper-methylation of the genome fail to maintain pluripotency at early passages. Human iPSCs are transgene-independently reprogrammed gradually through "convergence" of periodic aberrant hyper-methylation and become closer to ESCs upon continuous passaging. Due to the sensitivity to aberrant methylation on X chromosome, XY-iPSCs become close to ESCs faster than XX-iPSCs do.
doi:10.1371/journal.pgen.1002085.g007

did not resolve the aberrant hyper-methylation at MEG3-DMR, suggesting that these abnormalities occur at early passage and are fixed at later stages. In addition, aberrant hyper-methylation at *H19* in all iPSCs and ESCs was observed (Figure S10C), and *H19* was not expressed in all iPSCs and their parent cells.

We revealed that transgene-independent reprogramming is a convergence of periodic hyper-methylation. The aberrant hyper-methylation in iPSCs occurs stochastically throughout the genome. Early-stage iPSC clones with different propensities due to stochastic hyper-methylation may be used after selection of desirable phenotypes to treat a wide range of target diseases using cell-based therapy, and would thus have advantages for clinical use. In this sense, the number of ES-iPS-DMRs and methylation states of the stem cell-specific DMRs are useful epigenetic indices for evaluating human iPSCs in therapeutic applications.

Materials and Methods

Ethics statement

Human endometrium, amnion, placental artery endothelium and menstrual blood cells were collected by scraping tissues from surgical specimens, under signed informed consent, with ethical approval of the Institutional Review Board of the National Institute for Child Health and Development, Japan. Signed informed consent was obtained from donors, and the surgical specimens were irreversibly de-identified. All experiments handling human cells and tissues were performed in line with Tenets of the Declaration of Helsinki.

Human cell culture

Endometrium (UtE1104), amnion (AM936EP), placental artery endothelium (PAE551) and menstrual blood cell (Edom22) cell lines were independently established in our laboratory [41,42]. UtE1104, AM936EP, Edom22, and MRC-5 [43] cells were maintained in the POWEREDBY10 medium (MED SHIROTORI CO., Ltd, Tokyo, Japan). PAE551 cells were cultured in EGM-2MV BulletKit (Lonza, Walkersville, MD, USA) containing 5% FBS. Human iPSCs were generated in our laboratory, via procedures described by Yamanaka and colleagues [8] with slight modification [17,41,44–46]. The human cells were infected with retroviruses produced from the retroviral vector pMXs, which encodes the cDNA for human *OCT3/4*, *SOX2*, *c-MYC*, and *KLF4*. Human iPSCs were established from MRC-5, AM936EP, UtE1104, and PAE551, which were designated as MRC-iPSCs, AM-iPSCs, UtE-iPSCs and PAE-iPSCs [17,41,44–46]. Edom-iPSCs were established from Edom22 in this study. Human iPSCs were maintained on irradiated MEFs in 0222 medium (MED SHIROTORI CO., Ltd, Tokyo, Japan) supplemented with

10 ng/ml recombinant human basic fibroblast growth factor (bFGF, Wako Pure Chemical Industries, Ltd., Osaka, Japan). The 201B7 human iPSC line [8] that was generated from human skin fibroblasts by retroviral transfection with 4 transcription factors was also used. Frozen pellets of human ESCs (HUESCs) [23,24] were kindly gifted from Drs. C. Cowan and T. Tenzan (Harvard Stem Cell Institute, Harvard University, Cambridge, MA).

DNA methylation analysis

DNA methylation analysis was performed using the Illumina infinium assay with the HumanMethylation27 BeadChip (Illumina) and the BeadChip was scanned on a BeadArray Reader (Illumina), according to the manufacturer's instructions. Methylated and unmethylated signals were used to compute a β-value, which was a quantitative score of DNA methylation levels, ranging from "0", for completely unmethylated, to "1", for completely methylated. On the HumanMethylation27 BeadChip, oligonucleotides for 27,578 CpG sites covering more than 14,000 genes are mounted, mostly selected from promoter regions. CpG sites with ≥0.05 "Detection p value" (computed from the background based on negative controls) were eliminated from the data for further analysis, leaving 24,273 CpGs (13,728 genes) valid for use with the 51 samples tested. Average of methylation was calculated from HUESCs, MRC-iPSCs, AM-iPSCs, UtE-iPSCs, PAE-iPSCs and Edom-iPSCs, in which DMRs among each line in the each set were removed. Analyzed data sets (list of stem cell-specific DMRs and stem cell-required DMRs) can be obtained from http://www.nch.go.jp/reproduction/e/thdmds.html.

Gene expression analysis

Gene expression analysis was performed using the Agilent Whole Human Genome Microarray chips G4112F (Agilent, Santa Clara, CA), which contains over 41,000 probes. Raw data were normalized and analyzed by GeneSpringGX11 software (Silicon Genetics, Redwood City, CA). For RT-PCR, an aliquot of total RNA was reverse-transcribed using Random Hexamer primers. The cDNA template was amplified using specific primers for *EPHA1*, *PTPN6*, *RAB25*, *SALL4*, *GBP3*, *LYST*, *SP100*, *UBE1L*, OCT3/4 and NANOG. For detecting RNA derived from transgenes, specific primer sets, FY-11 and OCT3/4-SR, FY-11 and SOX2-SR, KLF4-SF and FY-12, cMYC-SF and FY-12, were used. Expression of glyceraldehyde-3-phosphate dehydrogenase (GAPDH) was used as a control. Primers used in this study are summarized in Table S8.

Quantitative combined bisulfite restriction analysis (COBRA) and bisulfite sequencing

To confirm the DNA methylation state, bisulfite PCR-mediated restriction mapping (known as the COBRA method) was performed. Sodium bisulfite treatment of genomic DNA was carried out using EZ DNA Methylation-Gold kit (Zymo Research). PCR amplification was performed using BIOTAQ HS DNA polymerase (Bioline Ltd; London, UK) with specific primers for *EPHA1*, *PTPN6*, *RAB25*, *SALL4*, *GBP3*, *LYST*, *SP100*, and *UBE1L*. Primers used in this study are summarized in Table S8. After digestion with restriction enzymes, HpyCH4IV or Taq I, quantitative-COBRA coupled with the Shimadzu MCE-202 MultiNA Microchip Electrophoresis System (Shimadzu, Japan) was carried out for quantitative DNA methylation level. To determine the methylation state of individual CpG sites, the PCR product was gel extracted and subcloned into pGEM T Easy vector (Promega, Madison, WI), and then sequenced. The promoter regions of the *OCT3/4* and *NANOG* [41,44] were also amplified and sequenced. Methylation sites were visualized and quality control was carried out by the web-based tool, "QUMA" (http://quma.cdb.riken.jp/) [47].

Web tools

The following web tools were used in this study: NIA Array [48] (http://lgsun.grc.nia.nih.gov/ANOVA/) for hierarchical clustering, DAVID Bioinformatics Resources [49] (http://david.abcc.ncifcrf.gov/home.jsp), PANTHER Classification System [50] (http://www.pantherdb.org/).

Accession numbers

NCBI GEO: HumanMethylation27 BeadChip data and gene expression microarray data have been submitted under accession number GSE 20750, GSE24676 and GSE24677.

Supporting Information

Figure S1 Immunohistochemistry of stem cell-specific surface antigens, NANOG, OCT3/4, SOX2, SSEA-4 and TRA-1-60 in AM-iPSCs, MRC-iPSCs and Edom-iPSCs, and teratoma formation of those iPSCs by subcutaneous implantation into NOD/Scid mice. The iPSCs differentiated to various tissues including ectoderm (neural tissues and retinal pigment epithelium), mesoderm (cartilage) and endoderm (gut). Immunostaining and teratoma formation were carried out as previously described [41,44].
(PDF)

Figure S2 Immunohistochemistry of stem cell-specific surface antigens, NANOG, OCT3/4, SOX2, SSEA-4 and TRA-1-60 in PAE-iPSCs and UtE-iPSCs, and teratoma formation of those iPSCs by subcutaneous implantation into NOD/Scid mice. The iPSCs differentiated to various tissues including ectoderm (neural tissues and retinal pigment epithelium), mesoderm (cartilage) and endoderm (gut). Immunostaining and teratoma formation were carried out as previously described [41,44].
(PDF)

Figure S3 Bisulfite sequencing at the OCT3/4 and NANOG promoter regions in ESCs, iPSCs and their parent cells.
(PDF)

Figure S4 Expression of the transgenes in iPSCs. (A) RT-PCR for transgenes in 22 iPSC lines. No expression of the transgenes in each iPSC lines was detected. (B) Quantitative RT-PCR for the transgenes at each passage. Relative expression of each transgene normalized to GAPDH was calculated. P0(D2), RNA from UtE1104 cells that were infected with the retroviruses and were cultured for 2 days. No expression of the transgenes at each passage was detected.
(PDF)

Figure S5 (A) Unsupervised hierarchical clustering analysis based on DNA methylation (left) and gene expression (right) in each ESC line, iPSC line and their parent cell line. (B) Unsupervised hierarchical clustering analysis based on DNA methylation (left) and gene expression (right) of average of ESCs, iPSCs and parent cells. (C) Scatter plot of DNA methylation (left) and gene expression data (right) in ESCs, iPSCs and their parent cells.
(PDF)

Figure S6 (A) Venn-like diagram showing seven categories (aa-gg) overlapped CpG sites among ESCs, iPSCs and their parent cells. (B) Number of CpG sites involved in each seven category from the five ESCs-iPSCs-the parent cell sets. "Overlapped"

indicates a number of sites that overlap in all iPSCs examined. The 220 overlapping sites in "ee" are designated as stem cell-specific differentially methylated regions (DMRs) and 3,123 total sites in "ee" are designated as stem cell-required DMRs. Notably, no overlapping sites were observed in "bb" that is a category involved in iPSCs-specific DMRs and in "ff" that is a category involved in inherited regions in iPSCs from the parent cells.
(PDF)

Figure S7 (A) Distribution of stem cell-required DMRs on each chromosome (upper) and frequency on each chromosome (bottom). (B) The number of parent cell specific DMRs (left) and the number of iPSC derived from different parent cells specific DMRs (left).
(PDF)

Figure S8 The number of DMRs between ESCs and each iPSC line (ES-iPS-DMRs) on each chromosome. ES-iPS-DMRs between 201B7 (iPSCs from Yamanaka) and ESCs are shown for comparison.
(PDF)

Figure S9 Distribution of the ES-iPS-DMRs on each chromosome. Distribution of the EiP-DMRs overlapped in less than 9 lines (light blue bars), in more than 10 and less than 14 lines (blue bars), and in more than 15 lines (red bars) among 22 lines.
(PDF)

Figure S10 DNA methylation at human *MEG3* and *H19*. (A) DNA methylation at MEG3-DMR (CG7) and expression of MEG3. (Top) Schematic diagram of the MEG3 gene. The arrow, open boxes and open circles represent transcription start site, first exon and position of CpG sites, respectively. Red and blue arrowheads represent the position of CpG sites in Infinium assay and COBRA assay, respectively. DNA methylation scores of MEG3 were determined by Illumina Infinium HumanMethylation27 assay (upper bar graph) and Bio-COBRA (lower bar graph). (Bottom) Expression of MEG3 and GAPDH was determined by RT-PCR. Information of MEG3 primers for COBRA and RT-PCR is described by Kagami et al. [40]. (B) Bisulfite sequencing analysis of MEG3-DMRs (CG7). (C) Methylation scores of H19 were determined by Illumina Infinium HumanMethylation27 assay.
(PDF)

Table S1 List of human cells analyzed for a methylation state in this study.
(PDF)

Table S2 STR analysis of iPSCs.
(PDF)

Table S3 Karyotypic analysis of iPSCs.
(PDF)

Table S4 List of genes with stem cell-specific DMRs exhibiting significant changes in expression in human iPS cells.
(PDF)

Table S5 List of the top 100 genes with hypo-methylated stem cell-required DMRs exhibiting 'high' expression in human iPS cells.
(PDF)

Table S6 List of top 100 genes with hyper-methylated stem cell-required DMRs exhibiting suppression in human iPS cells.
(PDF)

Table S7 List of top 5 categories of GO Term in "Stem cell-required DMRs".
(PDF)

Table S8 Primer list.
(PDF)

Acknowledgments

We would like to express our sincere thanks to Drs. C. Cowan and T. Tenzan for HUESC lines; to Drs. K. Hata and K. Nakabayashi for COBRA; to Dr. H. Makino for establishing the AM936EP, UtE1104, PAE551, and Edom22 cells; to Mr. M. Machida for immunohistochemical analysis; to Ms. Y. Takahashi for bioinformatics analyses; and Dr C. Ketcham for critical proofreading.

Author Contributions

Conceived and designed the experiments: KN AU. Performed the experiments: KN MT MY-I. Analyzed the data: KN. Contributed reagents/materials/analysis tools: KN MT MY-I YF EC HS HA. Wrote the paper: KN AU.

References

1. Li E (2002) Chromatin modification and epigenetic reprogramming in mammalian development. Nat Rev Genet 3: 662–673.
2. Reik W (2007) Stability and flexibility of epigenetic gene regulation in mammalian development. Nature 447: 425–432.
3. Feng S, Jacobsen SE, Reik W (2010) Epigenetic reprogramming in plant and animal development. Science 330: 622–627.
4. Hattori N, Nishino K, Ko YG, Ohgane J, Tanaka S, et al. (2004) Epigenetic control of mouse Oct-4 gene expression in embryonic stem cells and trophoblast stem cells. J Biol Chem 279: 17063–17069.
5. Hattori N, Imao Y, Nishino K, Ohgane J, Yagi S, et al. (2007) Epigenetic regulation of Nanog gene in embryonic stem and trophoblast stem cells. Genes Cells 12: 387–396.
6. Nishino K, Hattori N, Tanaka S, Shiota K (2004) DNA methylation-mediated control of Sry gene expression in mouse gonadal development. J Biol Chem 279: 22306–22313.
7. Zingg JM, Pedraza-Alva G, Jost JP (1994) MyoD1 promoter autoregulation is mediated by two proximal E-boxes. Nucleic Acids Res 22: 2234–2241.
8. Takahashi K, Tanabe K, Ohnuki M, Narita M, Ichisaka T, et al. (2007) Induction of pluripotent stem cells from adult human fibroblasts by defined factors. Cell 131: 861–872.
9. Yu J, Vodyanik MA, Smuga-Otto K, Antosiewicz-Bourget J, Frane JL, et al. (2007) Induced pluripotent stem cell lines derived from human somatic cells. Science 318: 1917–1920.
10. Park IH, Zhao R, West JA, Yabuuchi A, Huo H, et al. (2008) Reprogramming of human somatic cells to pluripotency with defined factors. Nature 451: 141–146.
11. Woltjen K, Michael IP, Mohseni P, Desai R, Mileikovsky M, et al. (2009) piggyBac transposition reprograms fibroblasts to induced pluripotent stem cells. Nature 458: 766–770.
12. Park IH, Arora N, Huo H, Maherali N, Ahfeldt T, et al. (2008) Disease-specific induced pluripotent stem cells. Cell 134: 877–886.
13. Miura K, Okada Y, Aoi T, Okada A, Takahashi K, et al. (2009) Variation in the safety of induced pluripotent stem cell lines. Nat Biotechnol 27: 743–745.
14. Ghosh Z, Wilson KD, Wu Y, Hu S, Quertermous T, et al. (2010) Persistent donor cell gene expression among human induced pluripotent stem cells contributes to differences with human embryonic stem cells. PLoS ONE 5: e8975. doi:10.1371/journal.pone.0008975.
15. Polo JM, Liu S, Figueroa ME, Kulalert W, Eminli S, et al. (2010) Cell type of origin influences the molecular and functional properties of mouse induced pluripotent stem cells. Nat Biotechnol 28: 848–855.
16. Kim K, Doi A, Wen B, Ng K, Zhao R, et al. (2010) Epigenetic memory in induced pluripotent stem cells. Nature.
17. Nishino K, Toyoda M, Yamazaki-Inoue M, Makino H, Fukawatase Y, et al. (2010) Defining Hypo-Methylated Regions of Stem Cell-Specific Promoters in Human iPS Cells Derived from Extra-Embryonic Amnions and Lung Fibroblasts. PLoS ONE 5: e13017. doi:10.1371/journal.pone.0013017.
18. Fazzari MJ, Greally JM (2004) Epigenomics: beyond CpG islands. Nat Rev Genet 5: 446–455.
19. Fazzari MJ, Greally JM (2010) Introduction to epigenomics and epigenome-wide analysis. Methods Mol Biol 620: 243–265.

20. Doi A, Park IH, Wen B, Murakami P, Aryee MJ, et al. (2009) Differential methylation of tissue- and cancer-specific CpG island shores distinguishes human induced pluripotent stem cells, embryonic stem cells and fibroblasts. Nat Genet 41: 1350–1353.
21. Lister R, Pelizzola M, Kida YS, Hawkins RD, Nery JR, et al. (2011) Hotspots of aberrant epigenomic reprogramming in human induced pluripotent stem cells. Nature 471: 68–73.
22. Bock C, Kiskinis E, Verstappen G, Gu H, Boulting G, et al. (2011) Reference Maps of Human ES and iPS Cell Variation Enable High-Throughput Characterization of Pluripotent Cell Lines. Cell 144: 439–452.
23. Cowan CA, Klimanskaya I, McMahon J, Atienza J, Witmyer J, et al. (2004) Derivation of embryonic stem-cell lines from human blastocysts. N Engl J Med 350: 1353–1356.
24. Osafune K, Caron L, Borowiak M, Martinez RJ, Fitz-Gerald CS, et al. (2008) Marked differences in differentiation propensity among human embryonic stem cell lines. Nat Biotechnol 26: 313–315.
25. Brena RM, Auer H, Kornacker K, Plass C (2006) Quantification of DNA methylation in electrofluidics chips (Bio-COBRA). Nat Protoc 1: 52–58.
26. Takahashi K, Yamanaka S (2006) Induction of pluripotent stem cells from mouse embryonic and adult fibroblast cultures by defined factors. Cell 126: 663–676.
27. Huangfu D, Osafune K, Maehr R, Guo W, Eijkelenboom A, et al. (2008) Induction of pluripotent stem cells from primary human fibroblasts with only Oct4 and Sox2. Nat Biotechnol 26: 1269–1275.
28. Fouse SD, Shen Y, Pellegrini M, Cole S, Meissner A, et al. (2008) Promoter CpG methylation contributes to ES cell gene regulation in parallel with Oct4/Nanog, PcG complex, and histone H3 K4/K27 trimethylation. Cell Stem Cell 2: 160–169.
29. Meissner A, Mikkelsen TS, Gu H, Wernig M, Hanna J, et al. (2008) Genome-scale DNA methylation maps of pluripotent and differentiated cells. Nature 454: 766–770.
30. Sato S, Yagi S, Arai Y, Hirabayashi K, Hattori N, et al. (2010) Genome-wide DNA methylation profile of tissue-dependent and differentially methylated regions (T-DMRs) residing in mouse pluripotent stem cells. Genes Cells 15: 607–618.
31. Chin MH, Pellegrini M, Plath K, Lowry WE (2010) Molecular analyses of human induced pluripotent stem cells and embryonic stem cells. Cell Stem Cell 7: 263–269.
32. Maherali N, Sridharan R, Xie W, Utikal J, Eminli S, et al. (2007) Directly reprogrammed fibroblasts show global epigenetic remodeling and widespread tissue contribution. Cell Stem Cell 1: 55–70.
33. Hall LL, Byron M, Butler J, Becker KA, Nelson A, et al. (2008) X-inactivation reveals epigenetic anomalies in most hESC but identifies sublines that initiate as expected. J Cell Physiol 216: 445–452.
34. Shen Y, Matsuno Y, Fouse SD, Rao N, Root S, et al. (2008) X-inactivation in female human embryonic stem cells is in a nonrandom pattern and prone to epigenetic alterations. Proc Natl Acad Sci U S A 105: 4709–4714.
35. Lengner CJ, Gimelbrant AA, Erwin JA, Cheng AW, Guenther MG, et al. (2010) Derivation of pre-X inactivation human embryonic stem cells under physiological oxygen concentrations. Cell 141: 872–883.
36. Tchieu J, Kuoy E, Chin MH, Trinh H, Patterson M, et al. (2010) Female human iPSCs retain an inactive X chromosome. Cell Stem Cell 7: 329–342.
37. Rugg-Gunn PJ, Ferguson-Smith AC, Pedersen RA (2005) Epigenetic status of human embryonic stem cells. Nat Genet 37: 585–587.
38. Rugg-Gunn PJ, Ferguson-Smith AC, Pedersen RA (2007) Status of genomic imprinting in human embryonic stem cells as revealed by a large cohort of independently derived and maintained lines. Hum Mol Genet 16 Spec No. 2: R243–251.
39. Stadtfeld M, Apostolou E, Akutsu H, Fukuda A, Follett P, et al. (2010) Aberrant silencing of imprinted genes on chromosome 12qF1 in mouse induced pluripotent stem cells. Nature 465: 175–181.
40. Kagami M, Sekita Y, Nishimura G, Irie M, Kato F, et al. (2008) Deletions and epimutations affecting the human 14q32.2 imprinted region in individuals with paternal and maternal upd(14)-like phenotypes. Nat Genet 40: 237–242.
41. Nagata S, Toyoda M, Yamaguchi S, Hirano K, Makino H, et al. (2009) Efficient reprogramming of human and mouse primary extra-embryonic cells to pluripotent stem cells. Genes Cells 14: 1395–1404.
42. Cui CH, Uyama T, Miyado K, Terai M, Kyo S, et al. (2007) Menstrual blood-derived cells confer human dystrophin expression in the murine model of Duchenne muscular dystrophy via cell fusion and myogenic transdifferentiation. Mol Biol Cell 18: 1586–1594.
43. Jacobs JP, Jones CM, Baille JP (1970) Characteristics of a human diploid cell designated MRC-5. Nature 227: 168–170.
44. Makino H, Toyoda M, Matsumoto K, Saito H, Nishino K, et al. (2009) Mesenchymal to embryonic incomplete transition of human cells by chimeric OCT4/3 (POU5F1) with physiological co-activator EWS. Exp Cell Res 315: 2727–2740.
45. Saito S, Onuma Y, Ito Y, Tateno H, Toyoda M, et al. (2010) Potential linkages between the inner and outer cellular states of human induced pluripotent stem cells. BMC Bioinformatics, in press.
46. Toyoda M, Yamazaki-Inoue M, Itakura Y, Kuno A, Ogawa T, et al. (2010) Lectin microarray analysis of pluripotent and multipotent stem cells. Genes Cells, in press.
47. Kumaki Y, Oda M, Okano M (2008) QUMA: quantification tool for methylation analysis. Nucleic Acids Res 36: W170–175.
48. Sharov AA, Dudekula DB, Ko MS (2005) A web-based tool for principal component and significance analysis of microarray data. Bioinformatics 21: 2548–2549.
49. Huang da W, Sherman BT, Lempicki RA (2009) Systematic and integrative analysis of large gene lists using DAVID bioinformatics resources. Nat Protoc 4: 44–57.
50. Mi H, Lazareva-Ulitsky B, Loo R, Kejariwal A, Vandergriff J, et al. (2005) The PANTHER database of protein families, subfamilies, functions and pathways. Nucleic Acids Res 33: D284–288.

THE JOURNAL OF BIOLOGICAL CHEMISTRY VOL. 286, NO. 13, pp. 11593–11603, April 1, 2011
© 2011 by The American Society for Biochemistry and Molecular Biology, Inc. Printed in the U.S.A.

A Distinct Role for Pin1 in the Induction and Maintenance of Pluripotency*

Received for publication, September 23, 2010, and in revised form, February 3, 2011 Published, JBC Papers in Press, February 4, 2011, DOI 10.1074/jbc.M110.187989

Mayuko Nishi,[a] Hidenori Akutsu,[b] Shinji Masui,[c] Asami Kondo,[a] Yoji Nagashima,[d] Hirokazu Kimura,[e] Kilian Perrem,[f] Yasushi Shigeri,[g] Masashi Toyoda,[b] Akiko Okayama,[h] Hisashi Hirano,[h] Akihiro Umezawa,[b] Naoki Yamamoto,[i] Sam W. Lee,[j] and Akihide Ryo[a1]

From the Departments of [a]Microbiology, [d]Pathology, and [h]Supramolecular Biology, Yokohama City University School of Medicine, Yokohama 236-0004, Japan, the [b]Department of Reproductive Biology, National Research Institute for Child Health and Development, Tokyo 157-8535, Japan, the [c]Department of Regenerative Medicine, Research Institute, International Medical Center of Japan, Tokyo 162-8655, Japan, the [e]Infectious Disease Surveillance Center, National Institute of Infectious Diseases, Tokyo 208-0011, Japan, the [f]Commonwealth Scientific and Industrial Research Organization, P.O. Box 225, Dickson, Australian Capital Territory 2602, Australia, the [g]National Institute of Advanced Industrial Science and Technology, Osaka 563-8577, Japan, the [i]Department of Microbiology, National University of Singapore, 117597 Singapore, and the [j]Cutaneous Biology Research Center, Massachusetts General Hospital and Harvard Medical School, Charlestown, Massachusetts 02129

The prominent characteristics of pluripotent stem cells are their unique capacity to self-renew and pluripotency. Although pluripotent stem cell proliferation is maintained by specific intracellular phosphorylation signaling events, it has not been well characterized how the resulting phosphorylated proteins are subsequently regulated. We here report that the peptidyl-prolyl isomerase Pin1 is indispensable for the self-renewal and maintenance of pluripotent stem cells via the regulation of phosphorylated Oct4 and other substrates. Pin1 expression was found to be up-regulated upon the induction of induced pluripotent stem (iPS) cells, and the forced expression of Pin1 with defined reprogramming factors was observed to further enhance the frequency of iPS cell generation. The inhibition of Pin1 activity significantly suppressed colony formation and induced the aberrant differentiation of human iPS cells as well as murine ES cells. We further found that Pin1 interacts with the phosphorylated Ser[12]-Pro motif of Oct4 and that this in turn facilitates the stability and transcriptional activity functions of Oct4. Our current findings thus uncover an atypical role for Pin1 as a putative regulator of the induction and maintenance of pluripotency via the control of phosphorylation signaling. These data suggest that the manipulation of Pin1 function could be a potential strategy for the stable induction and proliferation of human iPS cells.

Stem cells are characterized by their ability to self-renew through mitotic cell division and to differentiate into a diverse range of specialized cell types (1, 2). Human pluripotent stem cell proliferation is maintained through the action of several transcription factors including Oct4 (octamer 4), SOX2, Klf-4, Nanog, and c-Myc, which perform reprogramming functions under the stimulatory effects of stem cell-specific growth factors, including basic fibroblast growth factor (3–5). Basic fibroblast growth factor signaling has been shown to be essential for pluripotency as its depletion from cell culture media leads to aberrant cell differentiation and cell death (6, 7). Fibroblast growth factors produce mitogenic effects in targeted cells via signaling through cell surface receptor tyrosine kinases (8). These kinases can initiate intracellular signaling in cells, which is transmitted and diffused by tyrosine phosphorylation of the assembled proteins and of cellular substrates, including protein kinases with specificity for serine/threonine residues (8, 9). Although this intracellular phosphorylation signaling might indeed contribute to the self-renewal and pluripotency of stem cells (10, 11), it has not yet been fully determined how these phosphorylated proteins are further regulated.

Protein phosphorylation is a fundamental mode of intracellular signal transduction in a variety of key cellular processes such as cell proliferation, differentiation, and morphogenesis (12). A pivotal signaling mechanism that controls the function of phosphorylated proteins is the *cis-trans* isomerization of phosphorylated Ser/Thr-Pro motifs by the peptidylprolyl isomerase Pin1 (13, 14). This modification regulates multiple intracellular signaling pathways, including ErbB2/Ras, Wnt/β-catenin, and NF-κB, and thus plays an important role in the etiology of several human diseases (15–18). These include various cancers, Alzheimer disease, and immune disorders (14, 17, 18). However, the role of Pin1 in regulating the properties of pluripotent stem cells has not been adequately investigated to date.

In our current study, we investigated the role of Pin1 in the self-renewal and stemness of pluripotent stem cells. We reveal that Pin1 is induced upon cellular reprogramming and that its blockade significantly inhibits the self-renewal and maintenance of human iPS[2] cells in addition to murine ES cells. We find also that Pin1 can interact with phosphorylated Oct4 at the

* This work was supported in part by grants from the Takeda Science Foundation, Uehara Memorial Foundation, and Kanagawa Nanbyo Foundation (to A. R.).

[1] To whom correspondence should be addressed: Dept. of Microbiology, Yokohama City University School of Medicine, 3-9 Fuku-ura, Kanazawa-ku, Yokohama 236-0004, Japan. Tel.: 81-45-787-2602; Fax: 81-45-787-2851; E-mail: aryo@yokohama-cu.ac.jp.

[2] The abbreviations used are: iPS, induced pluripotent stem; AP, alkaline phosphatase; dnPin1, dominant-negative Pin1; 4F, four reprogramming factors; DMSO, dimethyl sulfoxide; SUMO, small ubiquitin-like modifier; Oct4, Octamer 4.

1000

Downloaded from www.jbc.org at Tokyo Ikashika Daigaku, on February 12, 2012

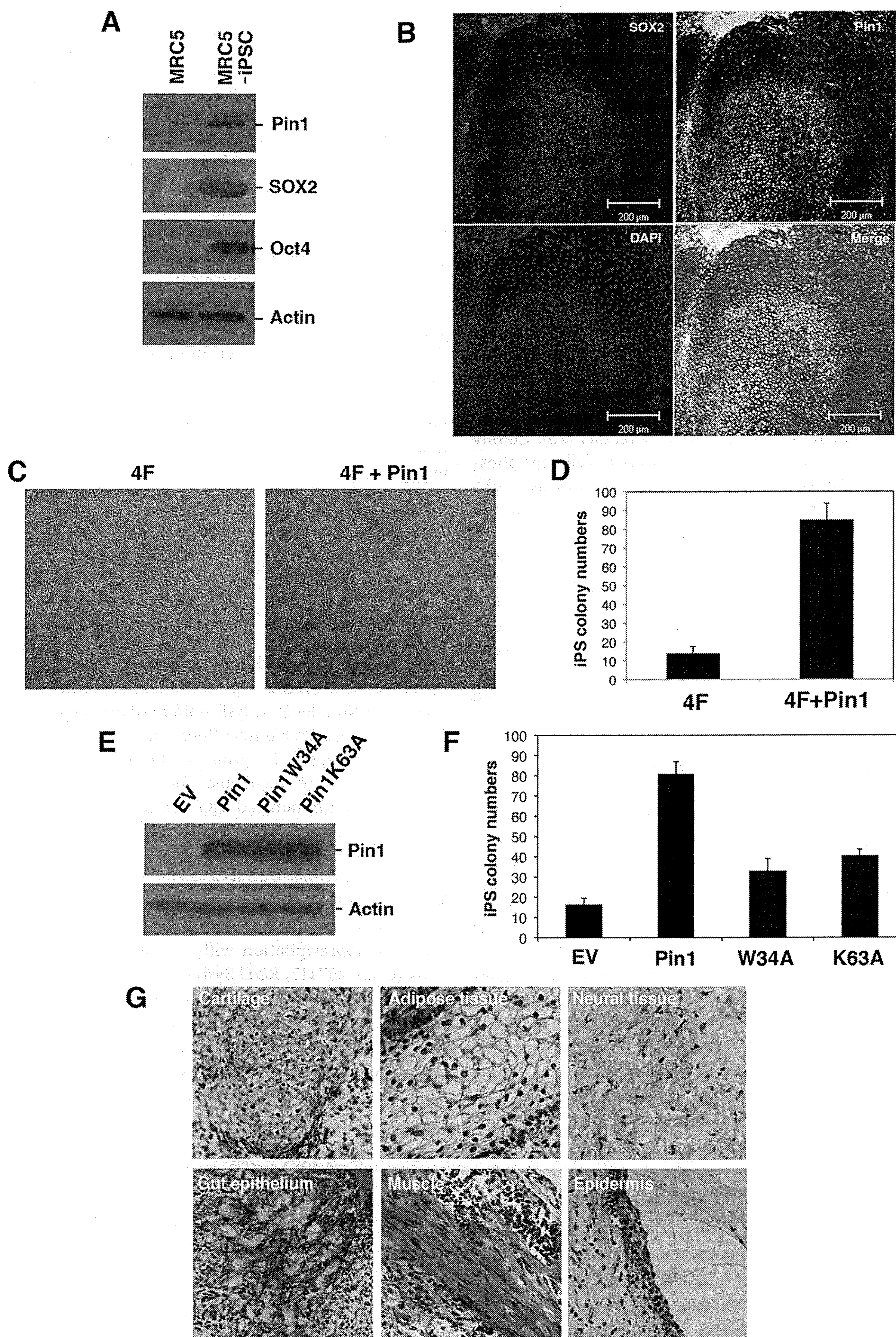

Downloaded from www.jbc.org at Tokyo Ikashika Daigaku, on February 12, 2012

Ser[12]-Pro motif in this protein. This enhances the stability and hence the transcriptional activity of Oct4. Our present data thus suggest that Pin1 is indeed a putative regulator of the self-renewal and proliferation of pluripotent stem cells.

EXPERIMENTAL PROCEDURES

Colony Formation Analysis—Human iPS cells were obtained from the RIKEN BioResource Center (clone no. 201B7) (19). Cells were cultured in human embryonic stem cell culture medium (KnockOut Dulbecco's modified Eagle's medium (Invitrogen)) supplemented with 20% KnockOut SR (Invitrogen), 1% GlutaMAX (Invitrogen), 100 μM nonessential amino acids (Invitrogen), 50 μM β-mercaptoethanol, and 10 ng/ml basic fibroblast growth factor). Murine ES cells were cultured in human embryonic stem cell culture medium (KnockOut Dulbecco's modified Eagle's medium supplemented with 15% KnockOut SR, 1% GlutaMAX (Invitrogen), 100 μM nonessential amino acids, 50 μM β-mercaptoethanol, and 1000 units/ml recombinant human leukemia inhibitory factor) (20). Colony formation was scored by counting the number of alkaline phosphatase (AP)-positive colonies as described previously (21). The number of cells per colony was determined by manually counting the number of DAPI-stained cells (21).

Cell Reprogramming—MRC5 fibroblasts were transduced with retroviral vectors encoding reprogramming factors as described previously (19). Briefly, the retroviral vector plasmids pMXs-hOct4, pMXs-hSOX2, pMXs-hKLF4, pMXs-hcMYC (Addgene), and pVSV-G were introduced into Plat-E cells using Effectene transfection reagent (Qiagen). After 48 h, virus-containing supernatants were passed through a 0.45-μm filter and supplemented with 10 μg/ml hexadimethrine bromide (polybrene). Cells were seeded at 6×10^5 cells per 60 mm dish at 24 h before incubation in the virus/polybrene-containing supernatants for 16 h. After 6 days, cells were plated on irradiated mouse embryonic fibroblasts, and culture medium was replaced with the hESC culture medium 24 h later. Cells were maintained at 37 °C and 5% CO_2 for 30 days.

Construction of Expression Vectors—Oct4 cDNA was subcloned into pcDNA3-HA expression vector (Invitrogen). Expression constructs of Oct4 were as follows: pcDNA-HA-Oct4 wild-type, amino acids 1–360; pcDNA-HA-Oct4 ΔC, amino acids 1–297; pcDNA-HA-Oct4 ΔN1, amino acids 138–360; pcDNA-HA-Oct4 ΔN2, amino acids 113–360; and pcDNA-HA-Oct4 ΔN3, amino acids 34–360. pcDNA-HA-Oct4-S12A was generated by KOD-Plus Mutagenesis Kit (Toyobo, Osaka, Japan) according to the manufacturer's instructions. The primers were 5′-CGCCCCCTCCAGGTGGT-3′ (forward) and 5′-CGAAGGCAAAATCTGAAGCC-3′ (reverse).

Gene Reporter Assay—A pGL3-fgf4 reporter plasmid containing an Oct-SOX binding cassette and the firefly luciferase gene was transfected with pRL-CMV (22). The −2601/+1 (nucleotide positions indicated with respect to the +1 translation start site) genomic fragment of the Oct4 promoter upstream region was amplified by PCR from human lymphocyte genomic DNA and cloned into the KpnI/HindIII sites of the pGL4-basic reporter plasmid (Promega, Madison, WI) as described previously (23). The primer sets were as follows: 5′-CCTGGTACCAGGATGGCAAGCTGAGAAACACTG-3′ and 5′-TCGCAAGCTTGCGAAGGGACTACTCAAC-3′. Cells were transfected with reporter plasmid vectors using Effectene (Qiagen) or Xfect Stem (Clontech). One day after transfection, the cells were resuspended in passive lysis buffer (Promega) and incubated for 15 min at room temperature. Luciferase activities were measured with a Dual-Luciferase reporter assay system (Promega) in accordance with the manufacturer's instructions.

GST Pulldown Assay and Immunoprecipitation Analysis—Cells were lysed with GST pulldown buffer (50 mM HEPES (pH 7.4), 150 mM NaCl, 10% glycerol, 1% Triton X-100, 1.5 mM $MgCl_2$, 1 mM EGTA, 100 mM NaF, 1 mM Na_3VO_4, 1 mM DTT, 5 μg/ml leupeptin, 1 μg/ml pepstatin, and 0.2 mM PMSF) and incubated with 30 μl of glutathione-agarose beads containing either GST-Pin1 or GST at 4 °C for 2 h. The precipitated proteins were then washed three times with lysis buffer and subjected to SDS-PAGE. For immunoprecipitation, cells were lysed with Nonidet P-40 lysis buffer (10 mM Tris HCl (pH 7.4), 100 mM NaCl, 0.5% Nonidet P-40, 1 mM Na_3VO_4, 100 mM NaF, 5 μg/ml leupeptin, 1 μg/ml pepstatin, and 0.2 mM PMSF). Cell lysates were incubated for 1 h with protein A/G-Sepharose·nonimmunized IgG complexes. Supernatant fractions were recovered and immunoprecipitated with 5 μg of anti-Myc antibody and 30 μl protein A/G-Sepharose. After washing three times with lysis buffer, the pellets were analyzed by SDS-PAGE.

Proteomics Analysis—Human iPS cell lysates were processed for immunoprecipitation with a monoclonal anti-Pin1 antibody (clone 257417, R&D Systems) at 4 °C for 3 h followed by SDS-PAGE. Gel lanes corresponding to the region from ~30 to 150 kDa were systematically excised, and the pieces were reduced, alkylated, and trypsinized. Peptides were analyzed by the linear ion trap Orbitrap hybrid mass spectrometer (Thermo Scientific). Protein identification was performed by peptide

FIGURE 1. **Pin1 is preferentially expressed in human iPS cells.** *A*, immunoblotting analysis of Oct4, SOX2, and Pin1 in MRC5 and MRC5-derived iPS cells. Actin was used as a loading control. *iPSC*, induced pluripotent stem cells; *EV*, empty vector. *B*, immunofluorescent analysis of Pin1 and SOX2 in human iPS cells. Representative images of phase-contrast microscopy and fluorescent immunocytochemistry for SOX2 (*red*) and Pin1 (*green*) are shown. Nuclei are indicated by DAPI staining (*blue*). Note that Pin1 is highly expressed in SOX2-positive pluripotent stem cells. *C* and *D*, Pin1 expression enhances 4F (Oct4, SOX2, Klf4, and c-Myc)-induced iPS cell induction. MRC5 fibroblasts were infected with retrovirus vectors encoding 4F and co-infected with those encoding either empty vector or Pin1. A representative picture of colony formations stained with AP is shown (*C*). The numbers of AP-positive colonies were scored in three independent experiments (*D*). Note that the co-introduction of Pin1 with 4F increases the frequency of iPS colony formation. *E* and *F*, MRC5 fibroblasts were infected with retrovirus vectors encoding 4F and co-infected with those encoding empty vector, HA-tagged wild-type Pin1, or its W34A or K63A mutants. The expression levels of HA-Pin1 or its mutants in infected MRC5 cells were analyzed by immunoblotting analysis with anti-HA antibody (*E*). The number of AP-positive colonies was scored in three independent experiments (*F*). *G*, teratoma tissue derived from human iPS cells induced by 4F and Pin1. iPS cells were transplanted subcutaneously into immunodeficient mice (2×10^6/mouse). Representative images of hematoxylin and eosin stained tumor with light microscope (200×) are shown.

Downloaded from www.jbc.org at Tokyo Ikashika Daigaku, on February 12, 2012

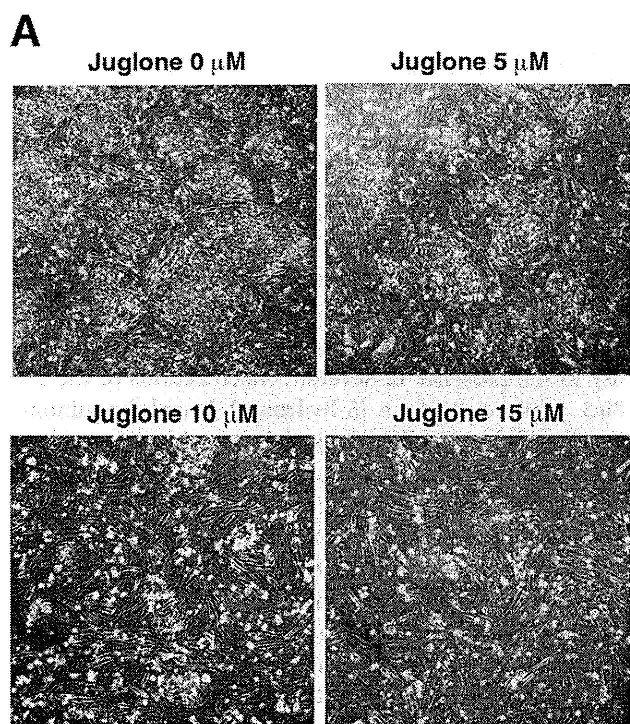

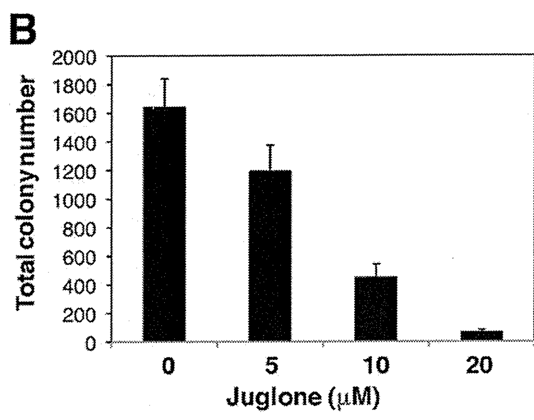

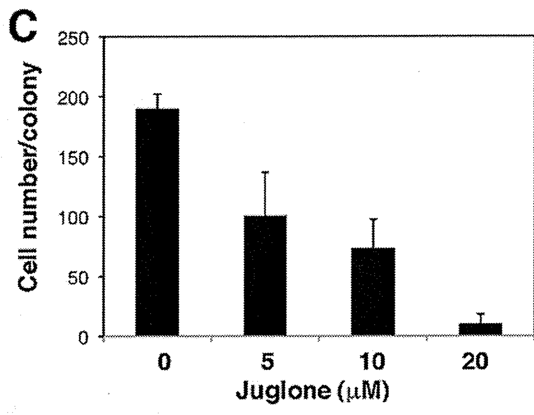

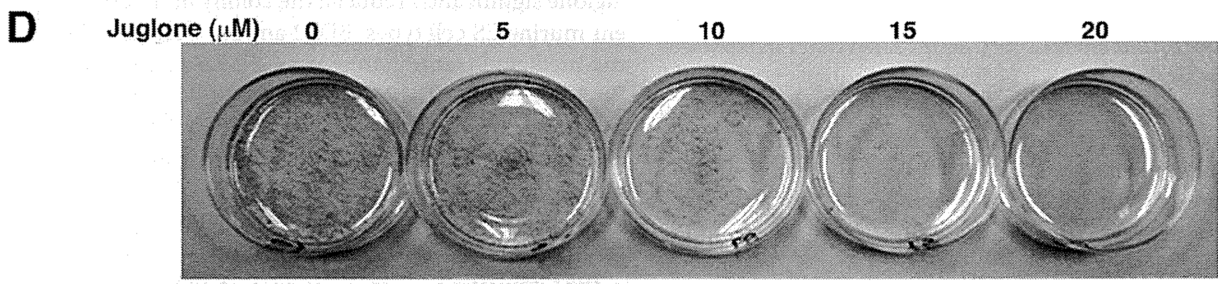

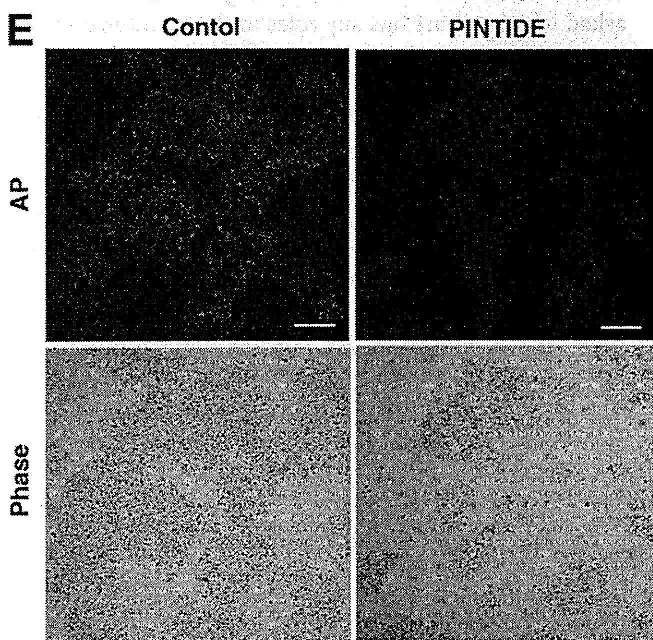

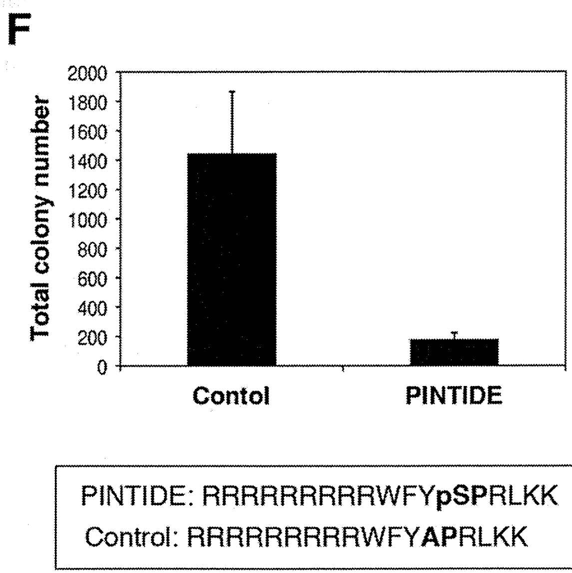

PINTIDE: RRRRRRRRRWFY**pSP**RLKK
Control: RRRRRRRRRWFY**AP**RLKK

Downloaded from www.jbc.org at Tokyo Ikashika Daigaku, on February 12, 2012

mass fingerprinting with the Mascot and Aldente search algorithms.

Quantitative Real-time PCR—Total RNA was extracted with TRIzol reagent (Invitrogen) according to the manufacturer's protocol. cDNA was synthesized using a cDNA synthesis kit (Toyobo, Osaka, Japan) and subjected to RT-PCR analysis with the SYBR Premix Ex gent Kit TaqII (Takara Bio, Shiga, Japan) using an Applied Biosystems 7300 real-time PCR System. The primer sets used were as follows: mOct4, 5′-CGTGTGAGGTGGAGTCTGGAGACC-3′ and 5′-ACTCGAACCACATCCTTCTCTAGCC-3′; mGAPDH, 5′-CCATGGAGAAGGCTGGGG-3′ and 5′-CAAAGTTGTCATGGATGACC-3′.

Teratoma Formation—Cells were harvested using accutase, collected into tubes, and centrifuged. The pellets were then suspended in human ESC culture medium. Fox Chase severe combined immunodeficiency mice (CREA, Tokyo, Japan) were injected with 2×10^6 cells mixed with an equal volume of Matrigel (BD Biosciences). Frozen tumor tissues embedded in optimum cutting temperature compound were sliced by cryosectioning and stained with hematoxylin and eosin.

RESULTS

Pin1 Is Induced upon Cellular Reprogramming and Enhances Generation of iPS Cells—To examine the role of Pin1 in cellular reprogramming and pluripotency, we initially investigated the expression levels of this prolyl isomerase in human iPS cells. Pin1 was found to be significantly induced upon the generation of iPS cells derived from MRC5 human fibroblasts (Fig. 1*A*). Immunofluorescent analysis further revealed that Pin1 is selectively expressed in SOX2-positive pluripotent stem cells, whereas its expression was found to be significantly suppressed in the surrounding SOX2-negative differentiated cells (Fig. 1*B*). These results indicate that Pin1 is preferentially expressed in reprogramming stem cells.

We next evaluated whether Pin1 affects the reprogramming of somatic cells into iPS cells. The co-infection of a Pin1-encoding retrovirus vector with those encoding four defined reprogramming factors (4F; SOX2, Oct4, Klf-4, and c-Myc) (24) notably boosted the generation of AP-positive iPS cell colonies compared with an induction of human fibroblast MRC5 cells with only four iPS factors (Fig. 1, *C* and *D*). We next performed a parallel experiment using either a WW-domain (binding domain) mutant (W34A) or a peptidyl prolyl isomerase-domain (catalytic domain) mutant (K63A) of Pin1. We confirmed the equivalent expression of each of these mutants and wild-type Pin1 (Fig. 1*E*). Neither of these mutants could boost iPS cell colony formation to the level seen with wild-type Pin1 (Fig. 1*F*), indicating that both the WW and PPIase domains are required for this function.

To test pluripotency *in vivo*, we transplanted 4F plus Pin1-introduced iPS cells subcutaneously into the dorsal flanks of immunodeficient mice. Nine weeks after injection, we observed teratoma formation composed of various tissues including gut-like epithelial tissues (endoderm), striated muscle (mesoderm), cartilage (mesoderm), neural tissues (ectoderm), and epidermal tissues (ectoderm) (Fig. 1*G*). These results indicate that the expression of Pin1 with defined reprogramming factors accelerates the frequency of iPS cell generation.

Pin1 Is Required for Pluripotent Stem Cell Self-renewal and Colony Formation—We next addressed whether Pin1 indeed plays any roles in the self-renewal of human iPS cells. iPS cells were dissociated with accutase and then plated at a clonal density in the presence of several concentrations of the selective Pin1 inhibitor juglone (5-hydroxy-1,4-naphthoquinone) (25, 26). The blockade of Pin1 by juglone considerably reduced both the numbers and size of the colonies in a dose-dependent manner (Fig. 2, *A–C*). It was notable also that the concentration of juglone used did not illicit nonspecific toxic effects in the feeder mouse embryonic fibroblast cells (Fig. 2*A* and data not shown). The effect of Pin1 inhibition upon colony formation was also confirmed in feeder-free cultures of human iPS cells by AP staining (Fig. 2*D*). Moreover, treatment with the Pin1 inhibitory phosphopeptide PINTIDE (27), but not a nonphosphorylated control peptide, significantly reduced the colony formation of human iPS cells (Fig. 2, *E* and *F*).

We next investigated the effects of Pin1 inhibition upon colony formation in murine ES cells. The blockade of Pin1 by juglone significantly reduced the colony numbers in two different murine ES cell types, BDF2 and R1 (Fig. 3*A*). The adenovirus-mediated transduction of a GFP-fused dominant-negative Pin1 (GFP-dnPin1) (28), but not a GFP control, significantly suppressed colony formation in murine ES (R1) cells manifesting as a considerable reduction in both the numbers and colony size of the murine ES cells (Fig. 3, *B–D*). These results together demonstrate that Pin1 is indispensable for the self-renewal and proliferation of pluripotent stem cells.

Pin1 Functions in Maintenance of Pluripotency—We next asked whether Pin1 has any roles in the maintenance of pluripotency in stem cells. Human iPS cells were dissociated and then cultured for 5 days to form colonies. When human iPS cells are cultured in hES medium supplemented with basic fibroblast growth factor, the overwhelming majority of the cells in the colonies are undifferentiated (Fig. 4*A*). However, treatment with juglone resulted in aberrant cell differentiation resulting in a "mosaic pattern" of iPS cell colonies following AP staining (Fig. 4*A*). Similarly, the adenovirus-mediated transduction of GFP-dnPin1, but not a GFP control, prominently reduced the number of AP-positive undifferentiated cells in murine ES cell colonies (Fig. 4*B*). These results together indicate that Pin1 can sustain pluripotent stem cells in an undifferentiated state in addition to the enhancement of self-renewal.

FIGURE 2. **Defective self-renewal of human iPS cells caused by Pin1 inhibition.** *A–C*, human iPS cells were dissociated with accutase and then plated on a feeder cell layer at a clonal density in the presence of the indicated concentrations of juglone for 3 days. Colony formation was analyzed by phase-contrast microscopy (*A*). The number of colonies was counted at 3 days after treatment (*B*). The number of cells per colony was determined by manually counting the DAPI-stained cells (*C*). Data are the mean ± S.E. *D*, human iPS cells were plated at a clonal density on the feeder-free culture in the presence of the indicated concentrations of juglone followed by AP staining. *E* and *F*, human iPS cells were dissociated with accutase and then plated on feeder-free dishes at a clonal density in the presence of 50 μg/ml of the Pin1 inhibitory phosphopeptide PINTIDE (RRRRRRRRRWFYpSPRLKK) or a nonphosphorylated control peptide (RRRRRRRRRWFYAPRLKK) for 48 h (*E*). AP-positive colony numbers were scored (*F*). Data are the mean ± S.E. *Scale bar*, 50 μm.

1004

Downloaded from www.jbc.org at Tokyo Ikashika Daigaku, on February 12, 2012

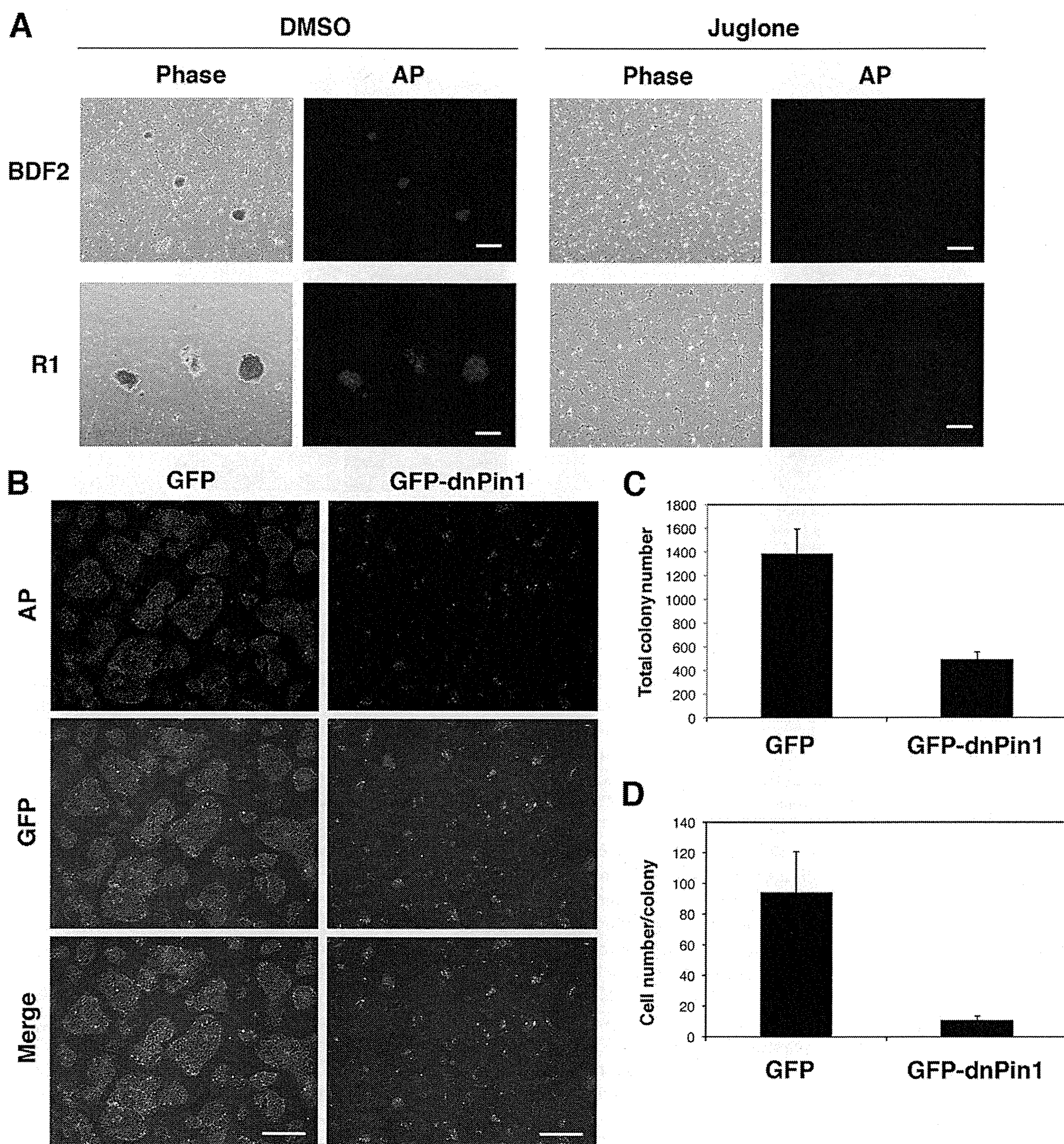

FIGURE 3. **Pin1 inhibition suppresses colony formation in murine ES cells.** *A*, two different murine ES cell types (BDF2 and R1) were plated on gelatin-coated dishes and treated with either DMSO or juglone (10 μM). Colonies were stained with AP (*red*). *Scale bar*, 200 μm. *B–D*, murine ES cells (R1) were infected with an adenovirus vector encoding either GFP or GFP-dnPin1 (3000 viral particles/cell). The cells were then stained with AP (*red*) and DAPI and analyzed by immunofluorescent microscopy (*B*). *Scale bar*, 200 μm. The total colony number (*C*) and the number of cells per colony (*D*) were then determined. Data are the mean ± S.E.

Identification of Pin1 Binding Proteins in Human iPS Cells—Our initial data indicated that Pin1 could enhance the function of reprogramming factors during the induction and maintenance of pluripotency. We next identified the substrates targeted by Pin1 in human iPS cells. Using a monoclonal Pin1 antibody, we co-immunoprecipitated proteins from human iPS cell lysates treated with a phosphatase inhibitor mixture. These isolated immune complexes were then boiled and resolved by one-dimensional SDS-PAGE, and the proteins were visualized using silver staining. Continuous regions of the gel corresponding to proteins of ~30 to 150 kDa in size were systematically excised (Fig. 5*A*), digested with trypsin, and analyzed in a linear

Downloaded from www.jbc.org at Tokyo Ikashika Daigaku, on February 12, 2012

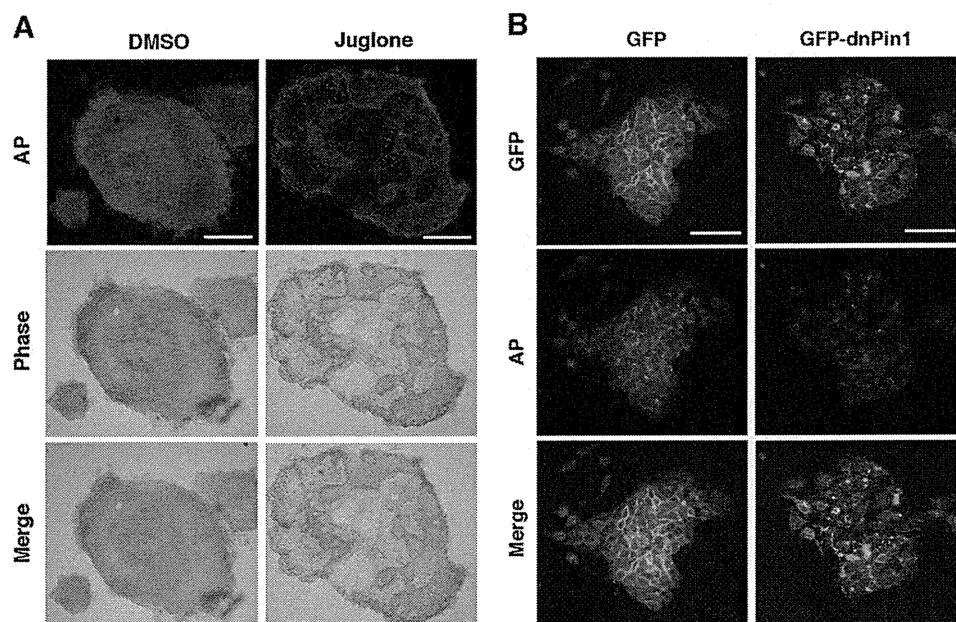

FIGURE 4. **Pin1 inhibition leads to the aberrant cell differentiation of human iPS cells.** *A*, human iPS cells were cultured for 5 days before forming colonies and then treated with either DMSO or juglone (10 μM) for 3 days. The cells were then stained with AP (*red*). Representative images of phase-contrast microscopy and fluorescent immunocytochemistry are shown. *Scale bar*, 200 μm. *B*, mouse ES cells were cultured for 2 days before forming colonies and then infected with an adenovirus vector encoding either GFP or GFP-dnPin1 (3000 viral particles/cell). After 48 h, the cells were then stained with AP (*red*) and DAPI (*blue*) and analyzed by immunofluorescent microscopy. *Scale bar*, 50 μm.

ion trap (LTQ) Orbitrap hybrid mass spectrometer. Peptide mass fingerprinting with the Mascot and Aldente search algorithms subsequently identified 23 Pin1 interacting proteins in human iPS cells (Fig. 5*B*). Notably, these Pin1-binding proteins included the pluripotent transcription factor Oct4. Because Oct4 has been shown to be a master regulator of pluripotency (29), we decided to further analyze the Oct4-Pin1 interaction.

Pin1 Binds and Regulates Protein Stability of Oct4—To further characterize the Oct4-Pin1 interaction, a GST pulldown analysis was initially performed. We found that recombinant GST-Pin1, but not GST alone, binds Oct4. This association was completely abolished by pretreatment of the cell lysates with calf intestine alkaline phosphatase (Fig. 6*A*), indicating that Pin1 binds phosphorylated Oct4. Immunofluorescence analysis further demonstrated that Pin1 co-localizes with Oct4 in the nuclei of iPS cells (Fig. 6*B*). Pin1 has been shown to regulate the stability of its substrate proteins upon binding (17), and we thus addressed whether this was the case for Oct4. Cycloheximide analysis using HeLa cells transfected with Oct4 alone or co-transfected with Oct4 and Pin1 revealed that the protein half-life of Oct4 is significantly enhanced in cells co-expressing Pin1 (Fig. 6*C*). Moreover, immunoprecipitation analysis with cells co-transfected with Oct4 and Myc-tagged ubiquitin, with or without Pin1 co-transfection, further revealed that Pin1 overexpression significantly reduces the polyubiquitination of the Oct4 protein (Fig. 6*D*). Consistently, the Oct4 protein expression level was significantly reduced in human iPS cells treated with juglone as compared with control cells (Fig. 6*E*). These results together confirm that Pin1 enhances the protein stability of Oct4 by suppressing ubiquitin proteasome-mediated proteolysis.

We next investigated the gene expression profile of Oct4 during the inhibition of Pin1. Murine ES cells were transfected with pGL4-Oct4-2601 promoter (harboring a genomic fragment of the Oct4 gene 5′-upstream region) and treated or not with juglone. Pin1 inhibition by juglone did not affect the transcriptional activity of the Oct4 promoter (Fig. 6*F*). Consistently, the results of parallel quantitative RT-PCR analysis demonstrated that the Oct4 mRNA level was not significantly altered by Pin1 inhibition (Fig. 6*G*), whereas the Oct4 protein level was significantly reduced by juglone treatment, as revealed by immunoblot analysis (Fig. 6*H*). These results together indicate that Pin1 regulates the protein stability of Oct4 but not Oct4 transcription.

We next addressed whether Pin1 enhances the transcriptional activity of the Oct4 protein. A luciferase reporter assay using the Oct-Sox enhancer region derived from the FGF4 gene was performed in HeLa cells co-transfected with Oct4, SOX2 or Pin1. Although the sole expression of Pin1 had no significant effects, the co-expression of Oct4 and Pin1 produced a significant increase in reporter activity in a dose-dependent fashion (Fig. 6*I*). This indicated that Pin1 promotes Oct4-mediated transcriptional activation. We performed a parallel experiment using the W34A and K63A Pin1 mutants. Neither of these mutants up-regulated the transcriptional activity of Oct4 to the levels seen with wild-type Pin1 (Fig. 6*J*), indicating that both the WW and PPIase domains are required for this function.

Pin1 Interacts with Ser^{12}-Pro motif of Oct4—To identify the specific Pin1 binding site within the Oct4 protein, we generated several Oct4 deletion mutants and performed GST-pulldown analysis. These experiments revealed that a C-terminal Oct4 deletion mutant (representing amino acids 1–297) could still bind Pin1, but that three extended N-terminal deletion mutants (amino acids 138–360, 113–360, or 34–360) failed to do so (Fig. 7*A*). These data indicate that Pin1 binds to Oct4 in the region between amino acids 1 and 34. Previous reports have indicated

Downloaded from www.jbc.org at Tokyo Ikashika Daigaku, on February 12, 2012

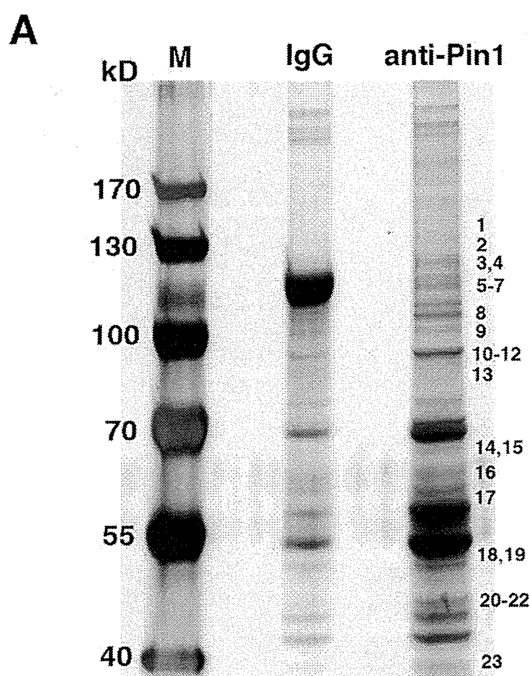

B

No.	Accession No.	Gene description	Predicted size
1	ADCY5_HUMAN	Adenylate cyclase type 5	138818
2	CCD40_HUMAN	Coiled-coil domain-containing protein 40	130033
3	PK3CA_HUMAN	Phosphatidylinositol-4,5-bisphosphate 3-kinase catalytic subunit alpha	124203
4	ZEB1_HUMAN	Zinc finger E-box-binding homeobox 1	123997
5	VINC_HUMAN	Vinculin	123722
6	RADIL_HUMAN	Ras-associating and dilute domain-containing protein	117351
7	UBP2L_HUMAN	Ubiquitin-associated protein 2-like	114465
8	DSG1_HUMAN	Desmoglein-1	113644
9	ENPP3_HUMAN	Ectonucleotide pyrophosphatase/phosphodiesterase family member 3	100059
10	ZN337_HUMAN	Zinc finger protein 337	86819
11	NASP_HUMAN	Nuclear autoantigenic sperm protein	85186
12	ZY11B_HUMAN	Protein zyg-11 homolog B	83921
13	MPEG1_HUMAN	Macrophage-expressed gene 1 protein	78587
14	FA13C_HUMAN	Protein FAM13C	65687
15	VPS45_HUMAN	Vacuolar protein sorting-associated protein 45	65036
16	ANR53_HUMAN	Ankyrin repeat domain-containing protein 53	59493
17	RPA34_HUMAN	DNA-directed RNA polymerase I subunit RPA34	54951
18	VIME_HUMAN	Vimentin	53619
19	KCAB1_HUMAN	Voltage-gated potassium channel subunit beta-1	46534
20	PRS8_HUMAN	26S protease regulatory subunit 8	45597
21	FKBP8_HUMAN	Peptidyl-prolyl cis-trans isomerase FKBP8	44534
22	PO5F1_HUMAN	POU domain, class 5, transcription factor 1 (OCT4)	38571
23	THAP1_HUMAN	THAP domain-containing protein 1	24928

FIGURE 5. **Identification of Pin1-binding proteins in human iPS cells.** *A* and *B*, lysates of human iPS cells were subjected to immunoprecipitation with either non-immunized control mouse IgG (IgG) or mouse anti-Pin1 monoclonal antibodies. Proteins bound to protein A/G-agarose beads were isolated, resolved by SDS-PAGE, and detected by silver staining (*A*). *M* indicates protein marker. Excised gel bands were digested with trypsin and analyzed on a linear ion trap (LTQ) Orbitrap hybrid mass spectrometer followed by peptide mass fingerprinting with the Mascot and Aldente search algorithms (*B*).

that Pin1 can bind only phosphorylated Ser/Thr-Pro motifs (17, 27) of which only one (Ser^{12}-Pro) exists between residues 1 and 34 in the Oct4 protein. Interestingly, this motif is conserved between various species including human, mouse, rat, and rabbit (Fig. 7*B*). We generated an Oct4 site-directed mutant at this site by substituting serine 12 for alanine (S12A). GST pulldown analysis subsequently revealed that Pin1 binds wild-type Oct4, but not its S12A mutant (Fig. 7*C*). These results confirm that Pin1 indeed bind the phosphorylated Ser^{12}-Pro motif of Oct4.

To further examine the functional interactions between Pin1 and Oct4 on this site, we next investigated the nature of the S12A mutant in terms of its protein expression in the presence of Pin1. HeLa cells were transfected with either wild-type Oct4 or its S12A mutant and co-transfected with Pin1. This was followed by immunoblotting analysis. We found that Pin1 increased the expression levels of wild-type Oct4, but not the S12A mutant (Fig. 7*D*).

DISCUSSION

In our present study, we report that Pin1 is an essential regulator of the self-renewal and maintenance of pluripotent stem cells. We further found the following: 1) Pin1 is induced upon the induction of human iPS cells; 2) the co-expression of Pin1 with defined reprogramming factors significantly enhances the

Downloaded from www.jbc.org at Tokyo Ikashika Daigaku, on February 12, 2012

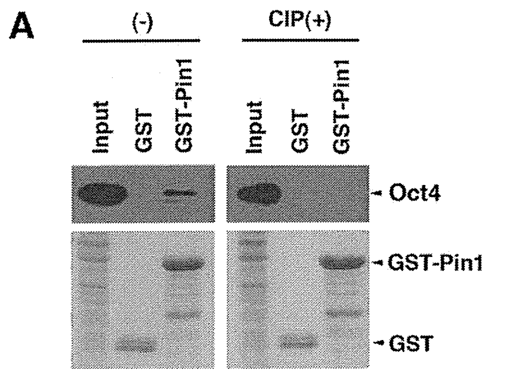

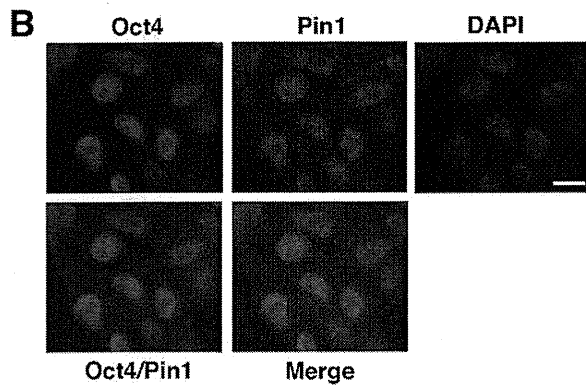

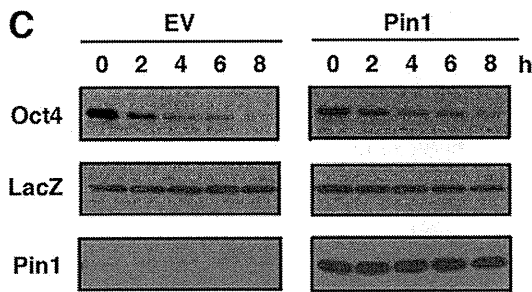

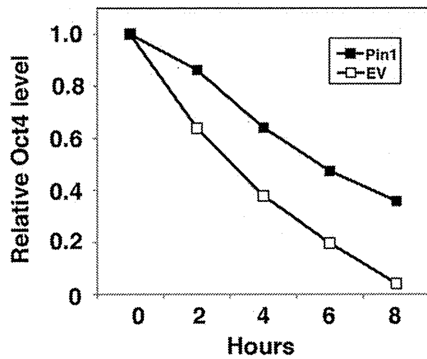

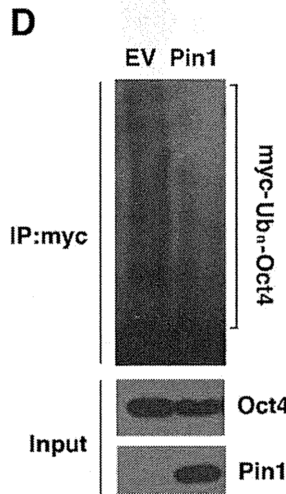

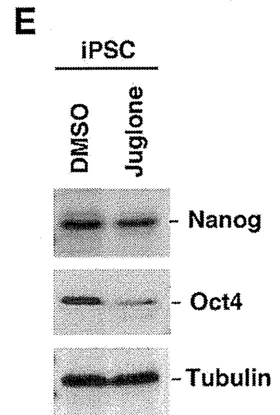

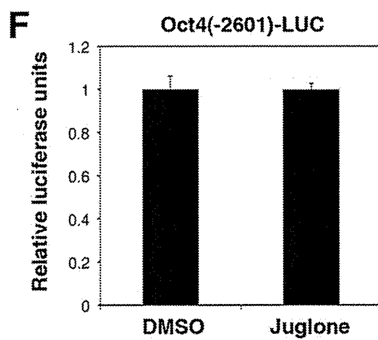

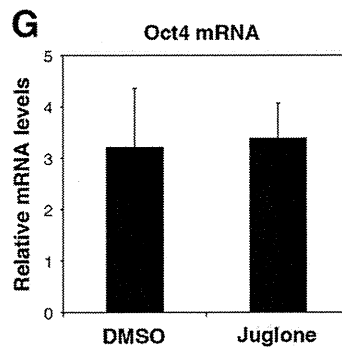

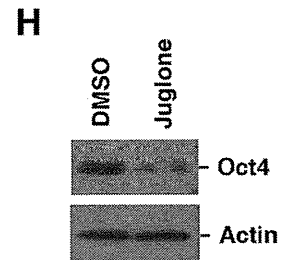

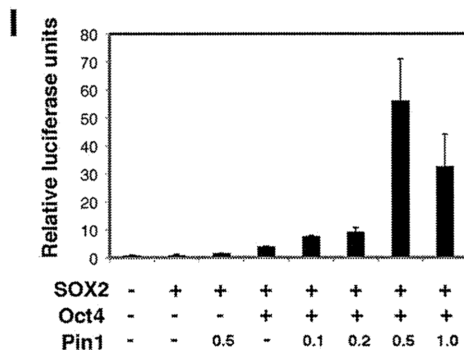

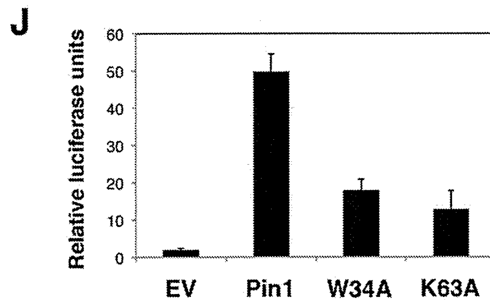

Downloaded from www.jbc.org at Tokyo Ikashika Daigaku, on February 12, 2012

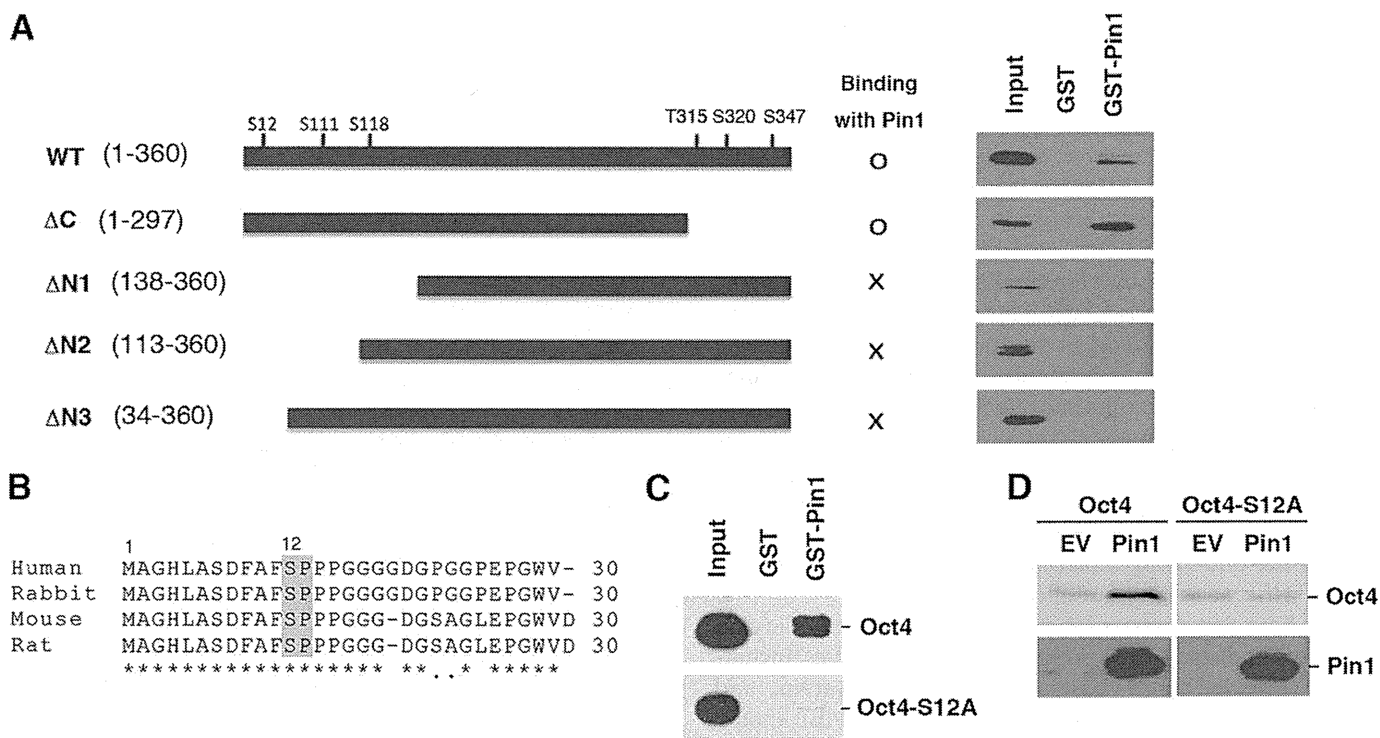

FIGURE 7. **Pin1 interacts with the Ser^{12}-Pro motif of Oct4.** *A*, schematic representation of the Oct4 deletion mutants generated in this study (*left panel*). HeLa cells were transfected with the indicated Oct4 deletion mutants for 24 h. Cell lysates were then prepared and subjected to GST pulldown analysis with either GST or GST-Pin1 followed by immunoblotting analysis with Oct4 antibodies (*right panel*). *B*, amino acid sequence alignment of the human, rabbit, mouse, and rat Oct4 proteins. The conserved Ser^{12}-Pro motifs are *boxed*. *C*, HeLa cells were transfected with the Oct4 site-directed mutant Oct4-S12A and subjected to GST pulldown analysis. *D*, HeLa cells were transfected with wild-type Oct4 or its S12A mutant with or without Pin1. After 24 h, the cells were subjected to immunoblotting analysis with an anti-Oct4 antibody.

frequency of iPS cell induction; 3) the blockade of Pin1 significantly inhibits the colony formation of dissociated human iPS cells and murine ES cells; 4) Pin1 inhibition leads to the aberrant cell differentiation in human iPS cells and murine ES cells after forming colonies; 5) Oct4 is a putative Pin1 substrate in human iPS cells; and 6) Pin1 interacts with Oct4 at its Ser^{12}-Pro motif and facilitates its stability and enhanced transcriptional activity. Our findings thus uncover a novel role of Pin1 as a putative regulator of the self-renewal and survival of pluripotent stem cells via Oct4 function.

Our current results add to previous findings indicating that Pin1 is a multifunctional protein that mediates various phosphorylated proteins involved in divergent cellular processes (17). This implicates Pin1 as a modulator of multiple signaling pathways depending on the cell type and biological context. Indeed, we demonstrate in our present study that Pin1 is a crucial regulator of the phosphorylation-dependent intracellular signaling network that controls cellular stemness and pluripotency. Moreover, iPS cells induced by the expression of four Yamanaka factors (Oct4, SOX2, Klf4, and c-Myc) led to a high expression level of Pin1, and these cells were found to be dependent on Pin1 function. This suggests that Pin1 could be one of the crucial factors in the induction of iPS cells from somatic cells that functions by cooperating with reprogramming transcription factors.

FIGURE 6. **Pin1 interacts with phosphorylated Oct4 and enhances its transcriptional activity.** *A*, human iPS cell lysates treated or untreated with calf intestine alkaline phosphatase were subjected to GST pulldown analysis with either GST or GST-Pin1, followed by immunoblotting analysis with anti-Oct4 antibody (*upper panel*). Coomassie staining for the GST or GST-Pin1 used in the assay is shown in the *lower panel*. *B*, human iPS cells were fixed with 4% paraformaldehyde and then co-immunostained with monoclonal antibodies against Oct4 (*green*) and polyclonal antibodies against Pin1 (*red*). Cells were then analyzed by confocal microscopy. *Scale bar*, 10 μm. *C*, HeLa cells transfected with the indicated vectors and HA-LacZ cells were treated with cycloheximide and harvested at the indicated time points. This was followed by immunoblotting analysis with Oct4, Pin1, and HA antibodies (*upper panel*). Quantitative data are shown in the *lower panel*. *D*, HeLa cells were transfected with Myc-tagged ubiquitin, Oct4, and co-transfected with either empty vector (*EV*) or Pin1. Cells were then treated with MG-132 for 12 h, and lysates were prepared and immunoprecipitated with anti-Myc antibody followed by immunoblotting analysis with anti-Oct4 antibody. Total cell lysates prior to immunoprecipitation (input) were immunoblotted with anti-Pin1 or anti-Oct4 antibody. *E*, human iPS cells were plated on Matrigel-coated feeder-free dishes and treated with either DMSO or juglone (20 μM) for 24 h. Cell lysates were then processed for immunoblotting analysis with anti-Nanog, anti-Oct4, or anti-tubulin antibodies. *F*, a plasmid containing the luciferase (*LUC*) gene flanked with 2601 bp of the Oct4 5′-upstream region was transfected into murine ES cells. The resulting cells were cultured in Matrigel-coated feeder-free dishes and treated with either DMSO or juglone (10 μM) for 24 h, and analyzed by gene reporter assay. *G*, murine ES cells were cultured in Matrigel-coated feeder-free dishes and treated with either DMSO or juglone (10 μM) for 24 h. Total RNAs were then extracted and reverse-transcribed. These preparations were then subjected to quantitative RT-PCR analysis for Oct4. The transcript levels were normalized using GAPDH. *H*, murine ES cells were cultured in Matrigel-coated feeder-free dishes and treated with either DMSO or juglone (10 μM) for 24 h. Cell lysates were then processed for immunoblotting analysis with either anti-Oct4 or anti-β-actin antibody. *I*, HeLa cells were transiently transfected with plasmids encoding Oct4, SOX2, or Pin1 and co-transfected with Oct-SOX reporter gene and pRL-CMV. At 24 h post-transfection, the cells were collected and subjected to a gene reporter assay. *J*, HeLa cells were transiently transfected with an Oct-SOX reporter gene and co-transfected with plasmids encoding wild-type Pin1 or its W34A or K63A mutants, together with Oct4 and SOX2. At 24 h post-transfection, the cells were collected and subjected to a gene reporter assay.

Downloaded from www.jbc.org at Tokyo Ikashika Daigaku, on February 12, 2012

The molecular mechanisms underlying the regulation of Pin1 in the induction and maintenance of pluripotency are likely to be highly complex given that Pin1 interacts with multiple substrates in pluripotent stem cells, as revealed by our proteomics analysis. However, our current findings also indicate that Pin1 is involved in the growth and maintenance of pluripotency in stem cells through its phosphorylation-dependent prolyl isomerization of substrates such as Oct4. In this regard, a recent report by Moretto-Zita *et al.* (30) has demonstrated that Pin1 can also associate with another pluripotent transcription factor, Nanog, in murine ES cells and sustain the self-renewal and teratoma formation of these cells in immunodeficient mice. These results indicate that Pin1 is a crucial modulator of the transcription factor network governing cellular stemness. It is possible also that Pin1 could regulate this process by modulating the function of other substrates. Further studies of Pin1 function in stem cells at various stages might shed new light on the underlying molecular pathways and factors that control self-renewal and multipotency.

It has been demonstrated that Pin1 knock-out mice develop normally but display some proliferation abnormalities, including a decreased body weight, retinal degeneration, and impaired mammary gland development (31, 32). Pin1 knockout mice also exhibit testicular atrophy with a significantly impaired proliferation of primordial germ cells and the progressive loss of spermatogenic cells (33). These phenotypes can now be attributed to the impaired maintenance and proliferation of germ-related stem cells due to the loss of Pin1 function.

In many circumstances, Pin1 acts as either a repressor or an enhancer of the degradation of substrate proteins (15–17, 34). Our current data now additionally demonstrate that Pin1 can also prolong the protein half-life of Oct4, thereby enhancing its transcriptional activity. Oct4 has been shown to be regulated by post-translational modifications such as SUMOylation (35). Our current findings reveal that Oct4 is also regulated by phosphorylation and subsequent prolyl isomerization. Identification of the kinase(s) responsible for the association of Pin1 and Oct4 will enhance our understanding of the regulatory pathways that operate during and after the induction of pluripotency.

It is desirable to utilize pluripotent stem cells such as iPS cells for future regenerative medicine applications. However, there are already concerns surrounding the use of iPS cells in a clinical setting because prior studies have suggested that they are likely to develop cancers (4, 36). Our current findings suggest, however, that the Pin1 inhibition could effectively block the proliferation of iPS cells in an undifferentiated state. Pin1 could therefore act as a molecular switch that can reversibly control the proliferation and survival of iPS cells, thereby reducing the risk of cell transformation and tumor formation.

Acknowledgments—We are grateful to the Riken Bioresource Center for providing human iPS cells and MRC5 fibroblasts. We also thank M. Machida, A. Hosoda, and S. Yoshizaki for comments on the manuscript and critical discussions and S. Baba and T. Taniguchi for technical assistance.

REFERENCES

1. Thomson, J. A., Itskovitz-Eldor, J., Shapiro, S. S., Waknitz, M. A., Swiergiel, J. J., Marshall, V. S., and Jones, J. M. (1998) *Science* **282,** 1145–1147
2. Watt, F. M., and Hogan, B. L. (2000) *Science* **287,** 1427–1430
3. Lewitzky, M., and Yamanaka, S. (2007) *Curr. Opin. Biotechnol.* **18,** 467–473
4. Takahashi, K., and Yamanaka, S. (2006) *Cell* **126,** 663–676
5. Boyer, L. A., Lee, T. I., Cole, M. F., Johnstone, S. E., Levine, S. S., Zucker, J. P., Guenther, M. G., Kumar, R. M., Murray, H. L., Jenner, R. G., Gifford, D. K., Melton, D. A., Jaenisch, R., and Young, R. A. (2005) *Cell* **122,** 947–956
6. Eiselleova, L., Matulka, K., Kriz, V., Kunova, M., Schmidtova, Z., Neradil, J., Tichy, B., Dvorakova, D., Pospisilova, S., Hampl, A., and Dvorak, P. (2009) *Stem Cells* **27,** 1847–1857
7. Dvorak, P., Dvorakova, D., Koskova, S., Vodinska, M., Najvirtova, M., Krekac, D., and Hampl, A. (2005) *Stem Cells* **23,** 1200–1211
8. Li, J., Wang, G., Wang, C., Zhao, Y., Zhang, H., Tan, Z., Song, Z., Ding, M., and Deng, H. (2007) *Differentiation* **75,** 299–307
9. Sun, H., and Tonks, N. K. (1994) *Trends Biochem. Sci.* **19,** 480–485
10. Brill, L. M., Xiong, W., Lee, K. B., Ficarro, S. B., Crain, A., Xu, Y., Terskikh, A., Snyder, E. Y., and Ding, S. (2009) *Cell Stem Cell* **5,** 204–213
11. Prudhomme, W., Daley, G. Q., Zandstra, P., and Lauffenburger, D. A. (2004) *Proc. Natl. Acad. Sci. U.S.A.* **101,** 2900–2905
12. Hunter, T. (2009) *Curr. Opin. Cell Biol.* **21,** 140–146
13. Lu, K. P., Hanes, S. D., and Hunter, T. (1996) *Nature* **380,** 544–547
14. Ryo, A., Liou, Y. C., Lu, K. P., and Wulf, G. (2003) *J. Cell Sci.* **116,** 773–783
15. Ryo, A., Suizu, F., Yoshida, Y., Perrem, K., Liou, Y. C., Wulf, G., Rottapel, R., Yamaoka, S., and Lu, K. P. (2003) *Mol. Cell* **12,** 1413–1426
16. Ryo, A., Nakamura, M., Wulf, G., Liou, Y. C., and Lu, K. P. (2001) *Nat. Cell Biol.* **3,** 793–801
17. Lu, K. P., and Zhou, X. Z. (2007) *Nat. Rev. Mol. Cell Biol.* **8,** 904–916
18. Esnault, S., Shen, Z. J., and Malter, J. S. (2008) *Crit. Rev. Immunol.* **28,** 45–60
19. Takahashi, K., Okita, K., Nakagawa, M., and Yamanaka, S. (2007) *Nat. Protoc.* **2,** 3081–3089
20. Yamada, M., Hamatani, T., Akutsu, H., Chikazawa, N., Kuji, N., Yoshimura, Y., and Umezawa, A. (2010) *Hum. Mol. Genet.* **19,** 480–493
21. Liu, Y., and Labosky, P. A. (2008) *Stem Cells* **26,** 2475–2484
22. Masui, S., Nakatake, Y., Toyooka, Y., Shimosato, D., Yagi, R., Takahashi, K., Okochi, H., Okuda, A., Matoba, R., Sharov, A. A., Ko, M. S., and Niwa, H. (2007) *Nat. Cell Biol.* **9,** 625–635
23. Yang, H. M., Do, H. J., Oh, J. H., Kim, J. H., Choi, S. Y., Cha, K. Y., Chung, H. M., and Kim, J. H. (2005) *J. Cell. Biochem.* **96,** 821–830
24. Takahashi, K., Ichisaka, T., and Yamanaka, S. (2006) *Methods Mol. Biol.* **329,** 449–458
25. Hennig, L., Christner, C., Kipping, M., Schelbert, B., Rücknagel, K. P., Grabley, S., Küllertz, G., and Fischer, G. (1998) *Biochemistry* **37,** 5953–5960
26. Shen, Z. J., Esnault, S., Schinzel, A., Borner, C., and Malter, J. S. (2009) *Nat. Immunol.* **10,** 257–265
27. Yaffe, M. B., Schutkowski, M., Shen, M., Zhou, X. Z., Stukenberg, P. T., Rahfeld, J. U., Xu, J., Kuang, J., Kirschner, M. W., Fischer, G., Cantley, L. C., and Lu, K. P. (1997) *Science* **278,** 1957–1960
28. Lu, P. J., Zhou, X. Z., Liou, Y. C., Noel, J. P., and Lu, K. P. (2002) *J. Biol. Chem.* **277,** 2381–2384
29. Niwa, H., Miyazaki, J., and Smith, A. G. (2000) *Nat. Genet.* **24,** 372–376
30. Moretto-Zita, M., Jin, H., Shen, Z., Zhao, T., Briggs, S. P., and Xu, Y. (2010) *Proc. Natl. Acad. Sci. U.S.A.* **107,** 13312–13317
31. Fujimori, F., Takahashi, K., Uchida, C., and Uchida, T. (1999) *Biochem. Biophys. Res. Commun.* **265,** 658–663
32. Liou, Y. C., Ryo, A., Huang, H. K., Lu, P. J., Bronson, R., Fujimori, F., Uchida, T., Hunter, T., and Lu, K. P. (2002) *Proc. Natl. Acad. Sci. U.S.A.* **99,** 1335–1340
33. Atchison, F. W., and Means, A. R. (2003) *Biol. Reprod.* **69,** 1989–1997
34. Ryo, A., Hirai, A., Nishi, M., Liou, Y. C., Perrem, K., Lin, S. C., Hirano, H., Lee, S. W., and Aoki, I. (2007) *J. Biol. Chem.* **282,** 36671–36681
35. Zhang, Z., Liao, B., Xu, M., and Jin, Y. (2007) *FASEB J.* **21,** 3042–3051
36. Knoepfler, P. S. (2009) *Stem Cells* **27,** 1050–1056

Downloaded from www.jbc.org at Tokyo Ikashika Daigaku, on February 12, 2012

Genes to Cells

Lectin microarray analysis of pluripotent and multipotent stem cells

Masashi Toyoda[1], Mayu Yamazaki-Inoue[1], Yoko Itakura[2], Atsushi Kuno[2], Tomohisa Ogawa[3], Masao Yamada[3], Hidenori Akutsu[1], Yuji Takahashi[1], Seiichi Kanzaki[1], Hisashi Narimatsu[2], Jun Hirabayashi[2] and Akihiro Umezawa[1]*

[1]*Department of Reproductive Biology, National Institute for Child Health and Development, 2-10-1 Okura, Setagaya-ku, Tokyo 157-8535, Japan*

[2]*Research Center for Medical Glycoscience, National Institute of Advanced Industrial Science and Technology, AIST Tsukuba Central 2, Tsukuba, Ibaraki 305-8568, Japan*

[3]*GP BioSceinces Ltd, 1-3-3, Azamino-Minami, Aoba-ku, Yokohama, Kanagawa 225-0012, Japan*

Stem cells have a capability to self-renew and differentiate into multiple types of cells; specific markers are available to identify particular stem cells for developmental biology research. In this study, we aimed to define the status of somatic stem cells and the pluripotency of human embryonic stem (hES) and induced pluripotent stem (iPS) cells using a novel molecular methodology, lectin microarray analysis. Our lectin microarray analysis successfully categorized murine somatic stem cells into the appropriate groups of differentiation potency. We then classified hES and iPS cells by the same approach. Undifferentiated hES cells were clearly distinguished from differentiated hES cells after embryoid formation. The pair-wise comparison means based on 'false discovery rate' revealed that three lectins -*Euonymus europaeus* lectin (EEL), *Maackia amurensis* lectin (MAL) and *Phaseolus vulgaris* leucoagglutinin [PHA(L)]- generated maximal values to define undifferentiated and differentiated hES cells. Furthermore, to define a pluripotent stem cell state, we generated a discriminant for the undifferentiated state with pluripotency. The discriminant function based on lectin reactivities was highly accurate for judgment of stem cell pluripotency. These results suggest that glycomic analysis of stem cells leads to a novel comprehensive approach for quality control in cell-based therapy and regenerative medicine.

Introduction

Stem cells produce almost every tissue of the human body. In general, they have the ability to divide and self-renew and to differentiate into various cell types. Stem cells have varying degrees of differentiation potential: (i) totipotency (ability to form the embryo and the trophoblast of the placenta) like fertilized eggs (zygotes); (ii) pluripotency (ability to differentiate into almost all cells that arise from the three germ layers) like human embryonic stem (hES) cells and induced pluripotent stem (iPS) cells; (iii) multipotentiality (capability of producing a limited range of differentiated cell lineages upon their location) like most tissue-based stem cells; and (iv) unipotentiality (ability to generate one cell type) like cells such as the epidermal stem cells and the spermatogonial cells of the testis. That is, a hierarchy of stem cells exists. In addition, human ES cell lines show variation in differentiation propensity (Osafune *et al.* 2008). iPS cells, another type of pluripotent stem cell, have been generated from somatic cells of different origin by retroviral transduction of four transcription factors (Takahashi *et al.* 2007; Yu *et al.* 2007). The established iPS cells have a wider variety of differentiation ability and gene expression when compared to ES cells (Aoi *et al.* 2008; Lee *et al.* 2009; Kaichi *et al.* 2010). However, a small proportion of these stem cells sometimes show spontaneous differentiation during serial passage. Therefore, to realize the potential for iPS cells to be utilized for cell therapy and as a valuable tool for drug discovery, it is necessary to monitor the status of these stem cells and to define

Communicated by: Takashi Tada
**Correspondence*: umezawa@1985.jukuin.keio.ac.jp

DOI: 10.1111/j.1365-2443.2010.01459.x
© 2010 The Authors
Journal compilation © 2010 by the Molecular Biology Society of Japan/Blackwell Publishing Ltd.

their exact stage during processes of growth and/or differentiation.

Glycosylation is a critical post- or co-translational modification found in more than 50% of eukaryotic proteins (Budnik *et al.* 2006). Thus, the glycome, which represents the total set of glycans expressed in a cell, is believed to be information-rich, as it varies among cell types, stages of development and differentiation, and even in the malignant transformation processes (Varki 1993). Lectins have long been used as tools to characterize cell surface glycans, such as for blood-group typing, tissue staining, lectin-probed blotting and flow cytometry (Sharon & Lis 2004). The use of lectins in glycan profiling provides considerable advantages. A modern technology to discriminate glycan profiling is lectin microarray analysis, which is an emerging technology that enables ultrasensitive detection of multiplex lectin–glycan interactions (Angeloni *et al.* 2005; Kuno *et al.* 2005; Pilobello *et al.* 2005). The system developed by Kuno *et al.* (2005) is based on a unique principle, that is, the evanescent-field fluorescence-detection principle, which has been used extensively for biosensors to study real-time binding events on the glass slide surfaces. Thus, the evanescent-field methods have greater advantage to analyze relatively weak interactions between lectins and glycoproteins in a liquid phase at equilibrium. Furthermore, this method is applicable for the analysis of the physiological and pathological status of crude glycoproteins extracted from mammalian cells (Ebe *et al.* 2006; Kuno *et al.* 2008) and cell surfaces (Tateno *et al.* 2007). Although the number of probes in lectin microarray is much smaller than in mRNA expression arrays, lectin microarray analysis enables high-throughput and sensitive analysis of a large set of biological samples and provides a snapshot of cell profiling. In this study, we further developed lectin microarray technology to define the status of somatic and pluripotent stem cells. The glycan-based comprehensive approach promises to be of great value, complementing more established methods such as gene expression analysis and epigenetic analysis.

Results

Lectin microarray analysis of mouse mesenchymal cells

Mesenchymal stem cells are multipotent and therefore may be useful in cell-based therapy along with ES cells and iPS cells. Mesenchymal stem cell (MSC) lines [(9-15c), osteoblasts (KUSA-A1), chondroblasts (KUM5) and preadipocytes (H-1/A)] were established from mouse bone marrow and were shown to retain potency both *in vivo* and *in vitro* (Umezawa *et al.* 1991; Matsumoto *et al.* 2005; Sugiki *et al.* 2007). To investigate their carbohydrate structures, we carried out a lectin microarray analysis of the cell membrane proteins. We quantified lectin signal using 'Array-Pro Analyzer' software and calculated the average net intensities of three spots for each lectin on the chip (Fig. 1A). Experiments with each cell line were performed in triplicate or quadruplicate. Four mesenchymal cell lines with different potencies showed differential lectin reactivities. 9-15c MSCs showed strong reactivity to wheat germ agglutinin (WGA), *Lycopersicon esculentum* lectin (LEL), concanavalin A (ConA), *Sambucus nigra* agglutinin (SNA) and *Ricinus communis* agglutinin I (RCA120) (Fig. 1A and Fig. S1 in Supporting Information). These signal intensities by lectin microarray were consistent with mean fluorescent intensities by flow cytometric analysis (Fig. 1B). We then performed hierarchical clustering analysis and principal component analysis (PCA) on the signal values of each lectin (Fig. 1C, D). H-1/A preadipocytes can be distinguished by KUM5 chondroblasts by lectin reactivities of GSL1A4, GSL1B4, BPL, PWM and MPA (PC1 axis), and 9-15c MSCs can be distinguished by KUSA-A1 osteoblasts by SNA. These cell types were reproducibly categorized into independent distinct groups.

Lectin microarray analysis of human mesenchymal cells

Human MSCs harvested from a variety of tissues have the capability to differentiate into numerous tissue lineages despite the fact that they may have tissue-specific characteristics. To clarify relationship between the tissue-specific characters of mesenchymal cells and glycomics, we performed lectin microarray analysis (LecChip™: Fig. S1 in Supporting Information) of mesenchymal cells derived from various tissues (Fig. 2A). Signal intensities by lectin microarray were consistent with the mean fluorescent intensities analysis determined by flow cytometric analysis (Fig. 2B). Hierarchical clustering analysis showed that human embryonic carcinoma NCR-G3 cells were reproducibly categorized into an independent group (red color in Fig. 2C), which is distinct from a group of mesenchymal cells derived from a variety of tissues (green color in Fig. 2C). In mesenchymal cells, bone marrow-, placenta- and extra finger-derived mesenchymal cells were categorized into distinct groups labeled in yellow, orange and blue, respectively (Fig. 2C).

© 2010 The Authors
Journal compilation © 2010 by the Molecular Biology Society of Japan/Blackwell Publishing Ltd.

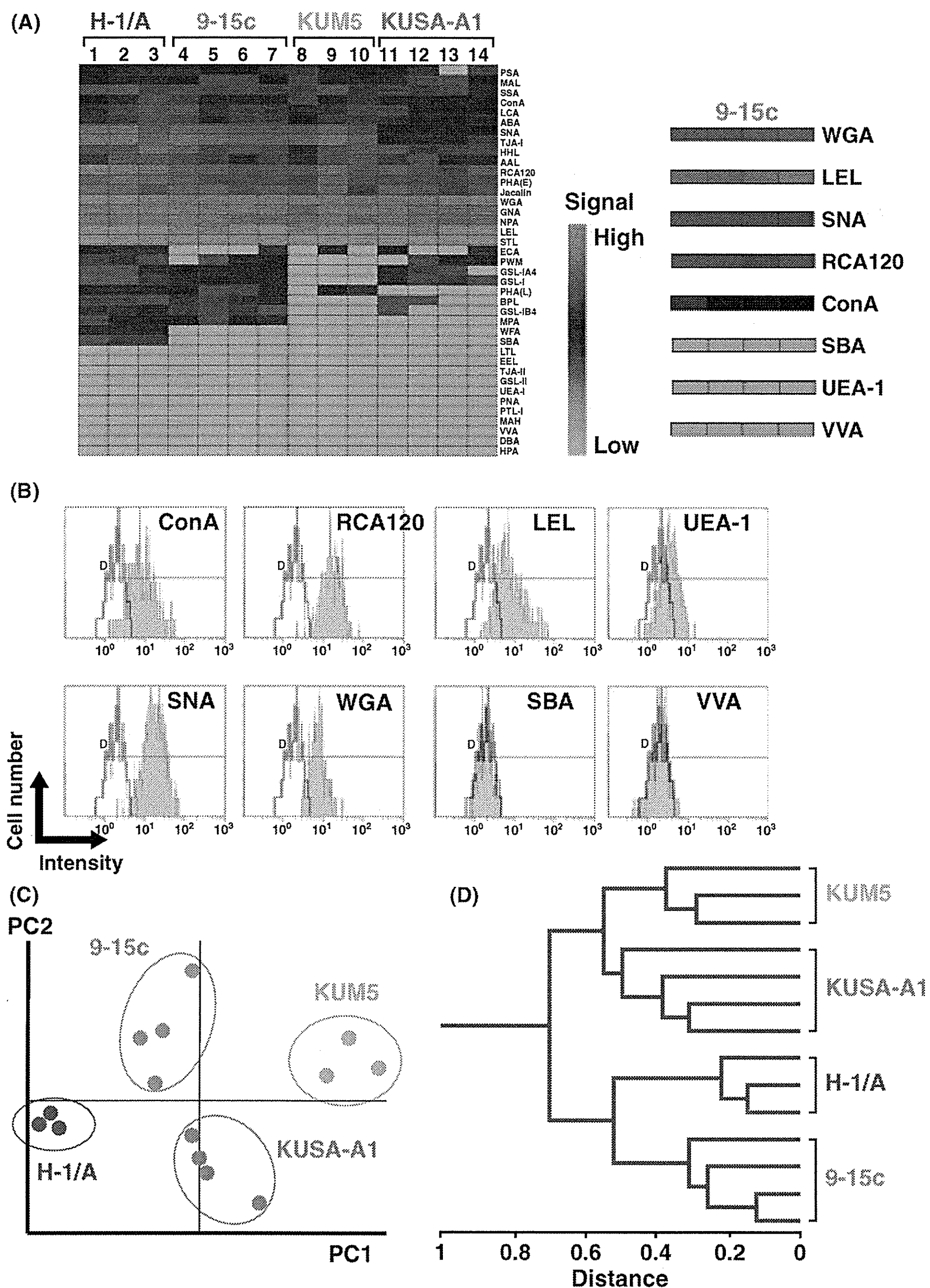

Figure 1 Lectin microarray analysis of mouse mesenchymal cells. (A) Heat map of 9-15c multipotent cells, KUSA-A1 osteoblasts, KUM5 chondroblasts and H-1/A preadipocytes. (B) Flow cytometric analysis of 9-15c multipotent cells using each lectin probe. Mean fluorescent intensities by flow cytometric analysis are consistent with signal intensities by lectin microarray. Nonshaded and shaded areas indicate reactivity of antibodies for isotype controls and that of antibodies for cell surface markers, respectively. (C) Principal component analysis of lectin microarray on mouse bone marrow–derived mesenchymal cells. Each cell is reproducibly subcategorized into groups of mesenchymal cell types. (D) Hierarchical clustering analysis of lectin microarray on mouse bone marrow–derived mesenchymal cells.

Human mesenchymal cells reacted to (i) *Pisum sativum* agglutinin (PSA), *Lens culinaris* agglutinin (LCA), *Aspergillus oryzae* lectin (AOL) and *Aleuria aurantia* lectin (AAL) that bind to Fucα1-6GlcNAc; (ii) SNA, *Sambucus sieboldiana* agglutinin (SSA) and *Trichosanthes japonica* agglutinin I (TJA-I) that bind to

© 2010 The Authors
Journal compilation © 2010 by the Molecular Biology Society of Japan/Blackwell Publishing Ltd.

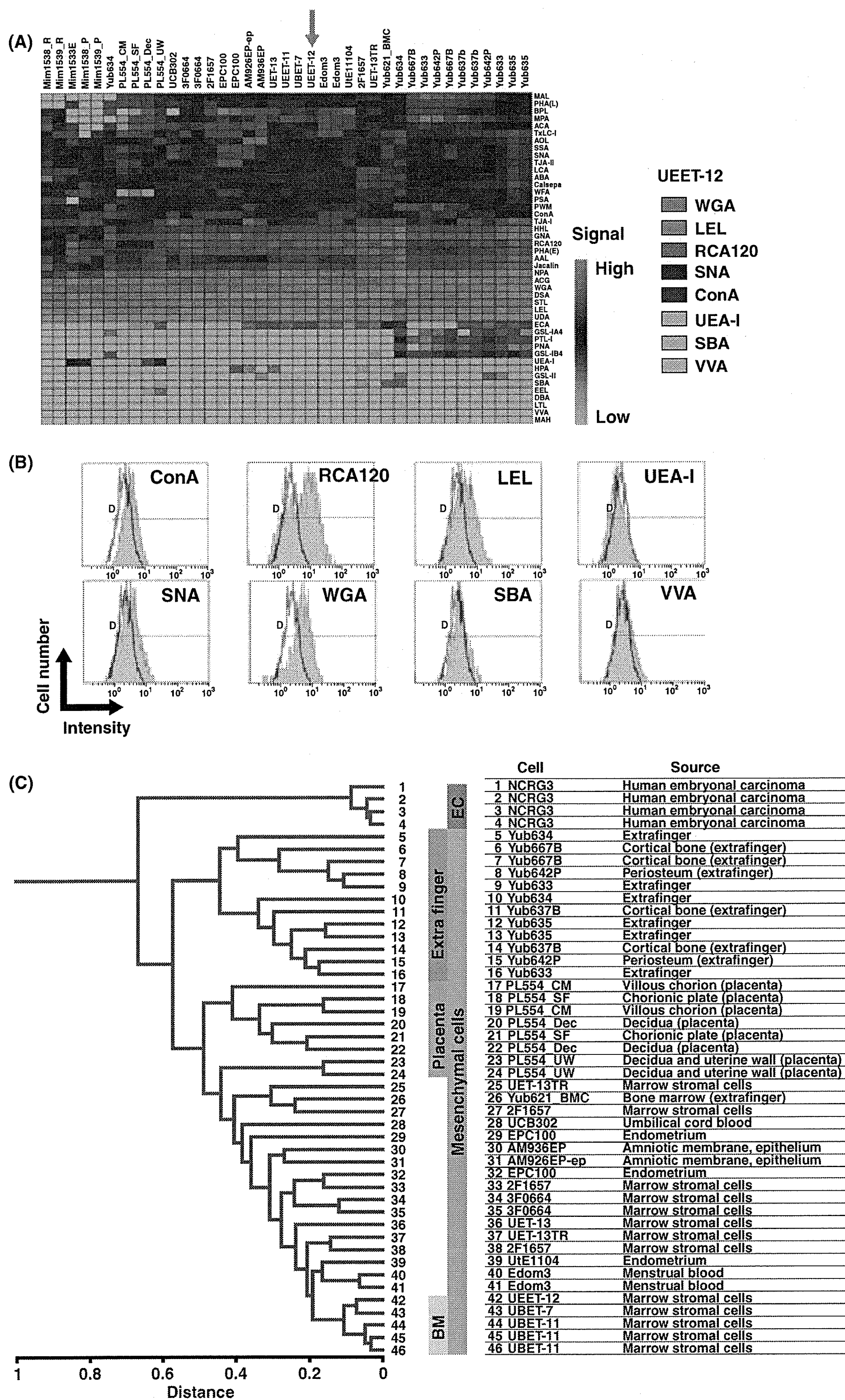

© 2010 The Authors
Journal compilation © 2010 by the Molecular Biology Society of Japan/Blackwell Publishing Ltd.